The Dissertation Committee for Windy Allman Certifies that this is the approved version of the following dissertation:

CELLULAR REQUIREMENTS FOR ANTIBODY PRODUCTION IN A NOVEL LPS-ENHANCED MODEL OF AUTOIMMUNE MYASTHENIA GRAVIS

Committee:

Premkumar Christadoss, M.D., Supervisor

Stephen Higgs, Ph.D.

Gary Klimpel, Ph.D.

Silvia Pierangali, M.D.

Socrates Tzartos, Ph.D.

Dean, Graduate School

Cellular Requirements for Antibody Production in a Novel LPS-enhanced Model of Autoimmune Myasthenia Gravis

by

Windy Allman, B.S.

Dissertation

Presented to the Faculty of the Graduate School of Biomedical Sciences

The University of Texas Medical Branch

in Partial Fulfillment of the Requirements

for the Degree of

Doctor of Philosophy

The University of Texas Medical Branch

December 2009

Dedication

To the many people and families affected by autoimmune diseases.

Acknowledgements

I would like to thank my research mentor, Dr. Premkumar Christadoss, for his support throughout my Ph.D. education. I have learned a great deal from the opportunities I had in his laboratory. I also would like to thank the members of the lab throughout the years (Shamsher Saini, Huibin Qi, and Jing Li) and my committee members (Dr. Gary Klimpel, Dr. Socrates Tzartos, Dr. Silvia Pierangeli, and Dr. Stephen Higgs) for their guidance. To my friends and family, thank you for your love and support throughout the years.

The completion of this dissertation was accelerated by the thoughtful discussions or with the kind assistance of the following people: Mark Griffin, Dr. Lynn Soong, Dr. Lijun Xin, Dr. Hakim Ben Nasr, Dr. Gregg Milligan, Dr. Lisa Elferink, Dr. Leopoldo Aguilera, Dr. Istvan Boldogh, Dr. Rahul Dasgupta, Nina Williams, and Peter German. I would like to give a special thank you to Dr. David Niesel, Dr. Rolf König, the Microbiology and Immunology department, and the Graduate School of Biomedical Sciences. I would like to express my appreciation to the Association Francaise contre les Myopathies (AFM) and the Myasthenia Gravis Foundation of America for their generous financial support of my studies.

Cellular Requirements for Antibody Production in a Novel LPS-enhanced Model of Autoimmune Myasthenia Gravis

Publication No._____

Windy R. Allman Ph.D.

The University of Texas Medical Branch, 2009

Supervisor: Premkumar Christadoss

Bacterial lipopolysaccharide (LPS) is a T cell-independent adjuvant known to abrogate peripheral tolerance. For the first time, the potential of LPS to induce antigen-specific B cell responses to acetylcholine receptor (AChR) in myasthenia gravis (MG) was evaluated in wild type (WT), CD4-/-, and CD8-/- C57BL/6 mice. Historically, MG has been induced in mice by immunization with AChR emulsified in complete Freund's adjuvant (CFA). WT mice immunized with AChR in LPS developed an MG-like disease (LPS-EAMG) similar to a disease induced by immunization with AChR in complete Freund's adjuvant (CFA-EAMG). The CD4-/- mice were resistant to the development of CFA-EAMG, but had significantly higher frequencies of IgG expressing AChR-binding B cells than WT mice. However, CFA-AChR immunization of CD4-/- mice failed to differentiate these cells to secrete anti-AChR IgG. The CD4-/- mice were susceptible to the development of LPS-EAMG and also had significantly higher frequencies of IgG expressing AChR-binding B cells than WT mice. WT and CD4-/- mice in the LPS-EAMG model had significant amounts of secreted high-affinity anti-AChR IgG2, immune complex deposits (IgG, C3, MAC) in muscle, and elevated sera levels of the B

cell survival factor, BAFF. Our results indicate that LPS abrogated B cell differentiation to antibody secreting cells in the LPS-EAMG model. Furthermore, CD8-/- mice were also susceptible to the development of LPS-EAMG, but were resistant to the development of moderate or severe signs of EAMG. While CD8 deficiency did not affect the quantity or avidity of secreted anti-AChR antibodies, it significantly reduced the survival of circulating IgG expressing AChR-binding B cells. The findings, accordingly have allowed us to identify an alternate cellular mechanism for the development of EAMG.

Table of Contents

LIST OF FIGURES xi

LIST OF ABBREVIATIONS xiii

CHAPTER 1: INTRODUCTION 1

- **MYASTHENIA GRAVIS** 1
- **PATHOGENESIS OF MG** 3
- **MATURATION OF ANTI-ACHR ANTIBODY RESPONSES** 4
- **EXPERIMENTAL AUTOIMMUNE MG** 8
- **THE ROLE OF INFECTION IN AUTOIMMUNITY** 8
- **OBJECTIVES OF THIS DISSERTATION** 11

CHAPTER 2: METHODS 13

- **INDUCTION OF MG** 13
- **MEASURING GRIP STRENGTH** 13
- **CLINICLAL EVALUATION OF EAMG** 14
- **CONJUGATION OF ALEXA FLUOR 647 TO ACHR** 14
- **BLOOD COLLECTION AND ALEXA FLUOR 647 LABELING OF CELLS** 15
- **DETECTION OF IGM, IGG2, C3, AND MAC DEPOSITS AT THE NMJ BY IMMUNOFLUORESCENCE MICROSCOPY** 15
- **ELISA FOR ANTI-ACHR ANTIBODIES AND AVIDITY** 16
- **FLOW CYTOMETRY OF LN CELLS** 17
- **RADIOIMMUNOASSAY FOR QUANTIFICATION OF ACHR IN MUSCLE** 17
- **ELISA FOR BAFF** 18

CHAPTER 3: BACTERIAL LIPOPOLYSACCHARIDE PROMOTED PROGRESSION OF EAMG 19
INTRODUCTION 19
RESULTS 20
LPS-ACHR IMMUNIZATION INDUCES EAMG IN C57BL/6 MICE LIKE THAT SEEN FOLLOWING CFA-ACHR IMMUNIZATION 20
LPS-ACHR IMMUNIZATION OF MICE LEADS TO SIGNIFICANT REDUCTION OF MUSCLE ACHR AND THE DEPOSITION OF IMMUNE COMPLEXES AT THE NMJ 24
DISCUSSION 28
CHAPTER 4: THE CHARACTERIZATION OF ACHR-SPECIFIC B CELLS BY FLOW CYTOMETRY 30
INTRODUCTION 30
RESULTS 31
DETECTION BY FLOW CYTOMETRY OF ACHR-BINDING B CELLS AMONG PBMCS OF MICE WITH EAMG 31
THE APPEARANCE AND FREQUENCY OF PERIPHERAL BLOOD ACHR-SPECIFIC B CELLS CORRELATES WITH THE SEVERITY OF EAMG 36
PLASMA SECRETED ANTI-ACHR IGS DO NOT CORRELATE WITH THE ACHR-SPECIFIC B CELL FREQUENCIES IN MICE WITH EAMG 38
DISCUSSION 40
CHAPTER 5: THE EFFECT OF CD4 DEFICIENCY ON ANTI-ACHR IG RESPONSES IN LPS-ACHR-INDUCED EAMG 43
INTRODUCTION 43
RESULTS 44
INDUCTION OF EAMG IN WT AND CD4-/- MICE 44
LPS-ACHR IMMUNIZED CD4-/- MICE PRODUCE SIGNIFICANT AMOUNTS OF CLASS-SWITCHED ANTI-ACHR ABS 49
LPS-ACHR IMMUNIZED CD4-/- MICE PRODUCE SIGNIFICANT AMOUNTS OF HIGH-AVIDITY ANTI-ACHR IGG2B ABS 49
LPS-ACHR IMMUNIZED CD4-/- MICE HAD INTENSE NMJ IGG2 AND C3 DEPOSITS 51

CD4-/- MICE HAVE ELEVATED FREQUENCIES OF ACHR-SPECIFIC IGG EXPRESSING PERIPHERAL BLOOD B CELLS 53

POTENTIAL ROLE OF ADJUVANT-INDUCED EXPRESSION OF CD40L AND BAFF IN DETERMINING B CELL DIFFERENTIATION 55

DISCUSSION 60

CHAPTER 6: THE EFFECT OF CD8 DEFICIENCY ON ANTI-ACHR IG RESPONSES IN LPS-ACHR-INDUCED EAMG 65

INTRODUCTION 65

RESULTS 66

LPS-ACHR IMMUNIZATION OF CD8-/- MICE INDUCES EAMG WITH REMISSION 67

CD8-/- MICE HAVE REDUCED FREQUENCIES OF PERIPHERAL BLOOD ACHR+IGG2+ B CELLS 70

DISCUSSION 73

CHAPTER 7: SUMMARY AND CONCLUSIONS 75

REFERENCES 78

VITA 93

List of Figures

Figure 1: **MECHANISMS OF ANTIBODY-MEDIATED DISRUPTION OF ACHR** 2

Figure 2: Current model of peripheral B lymphocyte differentiation 6

Figure 3: Grip strength ratio kinetics and sera anti-AChR Ab titers.....21

Figure 4: Comparison of kinetics and avidity of anti-AChR Ab production between CFA-AChR and LPS-AChR immunized mice.....23

Figure 5: LPS-AChR immunization of mice leads to loss of functional muscle AChR 25

Figure 6: Antibodies mediate muscle weakness of LPS-AChR immunized mice 26

Figure 7: TLR4 expression by I-A/I-E+ PBMCs 27

Figure 8: The characterization of AChR-binding peripheral blood lymphocytes by flow cytometry 32

Figure 9: Inhibition of Alexa fluor-AChR-binding peripheral blood B cells with unlabeled AChR.....34

Figure10: The kinetics on the frequencies of AChR-binding B cells 35

Figure 11: Correlation between AChR-binding peripheral blood B cells and markers of disease severity 37

Figure 12: Concentration of sera anti-AChR Igs does not correlate with the AChR-specific B cell frequencies 39

Figure 13: LPS-AChR immunized mice develop clinical signs of EAMG 45

Figure 14: LPS-AChR immunization of CD4-/- mice induces EAMG 47

Figure 15: Serum anti-AChR IgG and IgM responses in WT and CD4-/- mice after LPS-AChR immunization.....48

Figure 16: Kinetics and avidity of anti-AChR Abs by LPS-AChR immunized mice 50
Figure 17: IgG2 and C3 deposition at the NMJ 52
Figure 18: The frequencies of AChR-binding peripheral blood lymphocytes are elevated in CD4-/- mice 54
Figure 19: Flow cytometry analysis of T lymphocyte subsets and expression of CD40L 56
Figure 20: Lymph node T cell subsets and expression of CD40L on day 80 post immunization 57
Figure 21: Adjuvant-specific induction of BAFF and correlation with anti-AChR IgG2 secretion 59
Figure 22: A hypothetical model for the regulation of peripheral B cell tolerance in EAMG 62
Figure 23: CD8-/- mice are resistant to LPS-AChR induced EAMG 66
Figure 24: Sera anti-AChR IgG and IgM responses in WT and CD8-/- mice after LPS-AChR immunization 68
Figure 25: Avidity of anti-AChR IgM and IgG2 by LPS-AChR immunized WT and CD8-/- mice 69
Figure 26: IgG2, C3, and MAC deposition detected in muscle of CD8-/- immunized mice 71
Figure 27: The frequencies of AChR-binding peripheral blood B cells are reduced in CD8-/- mice 72

List of Abbreviations

Abs	Antibodies
AChR	Acetylcholine receptor
Ag	Antigen
AID	Activation-induced cytidine deaminase
APRIL	A proliferation-inducing ligand
BAFF	B-cell activating factor
BCR	B cell receptor
Btx	Bungarotoxin
CFA	Complete Freund's adjuvant
CSR	Class switch recombination
DCs	Dendritic cells
EAE	Experimental autoimmune encephalomyelitis
EAMG	Experimental autoimmune mysthenia gravis
EAT	Experimental autoimmune thyroiditis
FDC	Follicualr dendritic cell
GC	Germinal Center
IFA	Incomplete Freund's adjuvant
Ig	Immunoglobulin
IL	Interleukin
LN	Lymph node

LPS	Lipopolysaccharide
MAC	Membrane attack complex
MG	Myasthenia gravis
MHC	Major histocompatibility complex
MUSK	Muscle specific tyrosine kinase
MZB	Marginal zone B cell
NMJ	Neuromuscular junction
NOD	Non-obese diabetic
OVA	Ovalbumin
PBL	Peripheral blood lymphocyte
PBS	Phosphate-buffered saline
RIA	Radioimmunoassay
SH	Somatic Hypermutation
SLE	Systemic lupus erythematosis
TECs	Thymic epithelial cells
TLR4	Toll receptor 4
TNF	Tumor necrosis factor

Chapter 1: Introduction

MYASTHENIA GRAVIS

Myasthenia gravis (MG) is a chronic autoimmune condition characterized by fluctuating voluntary muscle weakness (1). Like many autoimmune diseases, the cause is unknown, but both genetic and environmental factors are thought to contribute to disease development (2). There are 200-400 cases of MG per million persons and the prevalence has been continually growing since the 1950's (3). The disease prevalence is higher in men with the average onset of age in the 50s. However, in women the disease often develop between the ages of 20- 40. Symptoms of MG are dependent upon the muscles affected, which vary significantly from patient to patient. However, the most frequent symptoms of MG are caused by weakness in the ocular and bulbar muscles, and include facial weakness, diplopia, ptosis, and difficulty in swallowing, chewing, and talking. Limb, trunk, and respiratory muscles may also be affected, causing fatigue and feelings of heaviness (4). Two-thirds of the patients initially present with the ocular muscle weakness (5). In 90% of the cases the disease will progress to other muscles of the body.

Various studies have confirmed that the symptoms of MG are caused by antibodies (Abs) interfering with cell signaling at the neuromuscular junction (NMJ) (6-8). Current therapies aim to prolong the lifespan of the neurotransmitter acetylcholine (cholinesterase inhibitors) and to suppress the immune system [steroids (prednisone or cyclosporine), thymectomy, plasma exchange, and intravenous immunoglobulin (IVIG)] (2). If the condition is left untreated, muscle atrophy may occur and may be fatal if

respiratory muscles are affected. With few patients going into remission, treatment is lifelong, expensive, and has potential side effects.

PATHOGENESIS OF MG

Muscle movement occurs by electrical depolarization of muscle membranes. The neurotransmitter, acetylcholine, is secreted by neurons and triggers the opening of the gated-ion channels acetylcholine receptors (AChR) thus depolarizing muscle membranes (Figure 1) (3, 4). Approximately 85% of patients have Abs specific for AChR (9, 10). Anti-AChR Abs interfere with neuromuscular transmission in three ways: destruction of postsynaptic AChR by complement activation (Figure 1A), antigenic modulation (Figure 1B), and inhibition of AChR function (Figure 1C). A subset of MG patients (7-10%), have anti-muscle specific tyrosine kinase (MUSK) Abs which mediate pathogenesis of MG by a different mechanism (11). Other auto-Abs found in MG patients include Ab directed against titin, myosin, actin, IFN-α, IL-12, and tropomysin (4). The role of some of these auto-Abs is unclear. The focus of this dissertation is on anti-AChR Ab positive MG and the mechanisms of production of anti-AChR Abs.

Patients with anti-AChR Abs are generally classified as either early-onset without thymoma (<50 years old), late-onset without thymoma (>40 years old), and patients with thymoma . Approximately 80% of MG patients have thymic abnormalities, such as thymitis, thymoma, or involusion (12). The thymus is considered by many to be the site

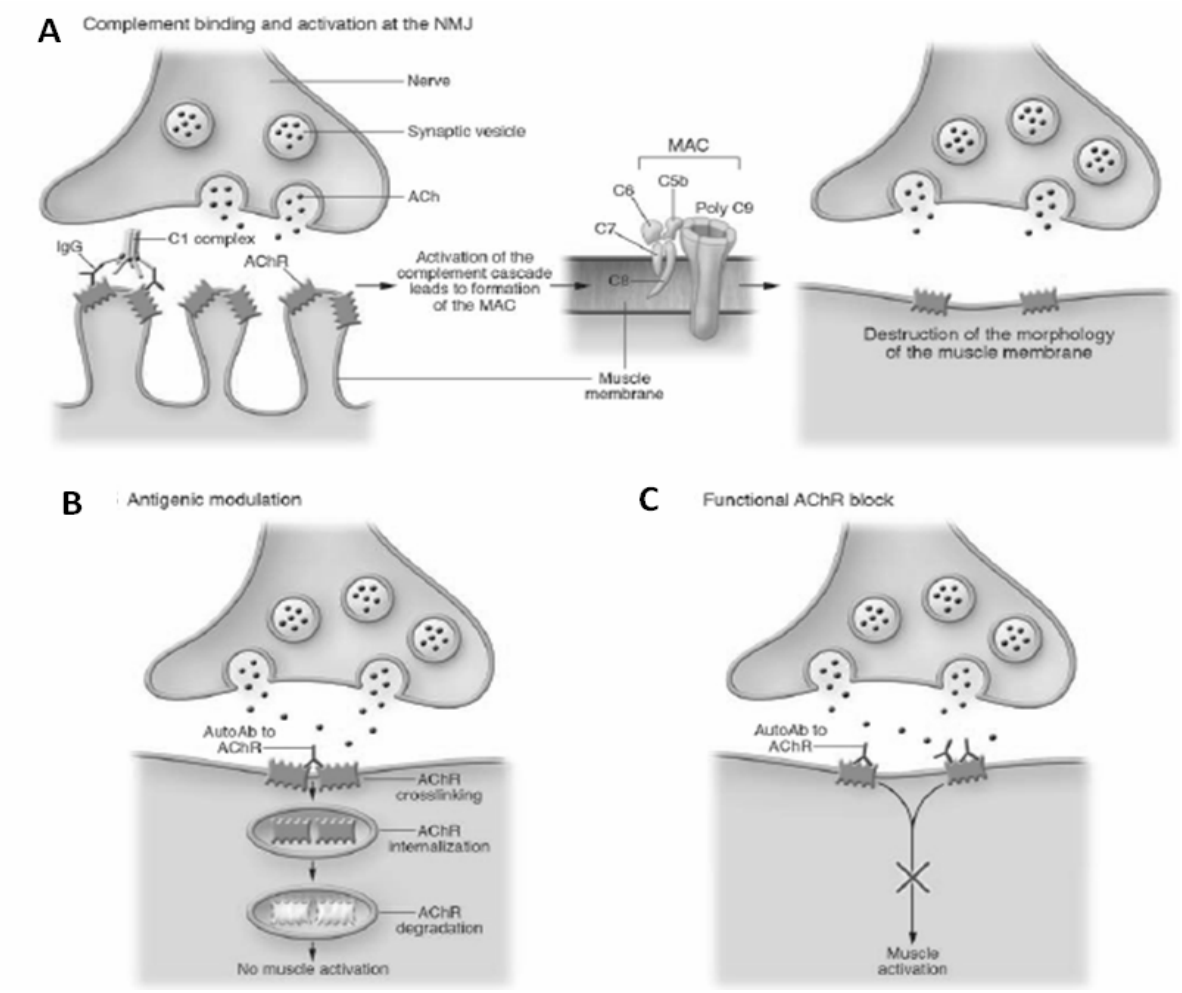

Figure 1: Mechanisms of antibody-mediated disruption of AChR. (A) Anti-AChR Abs bind to AChR and activate complement system culminating in the formation of MAC and the subsequent destruction of the postsynaptic NMJ membrane. (B) Anti-AChR Abs crosslink AChRs accelerating AChR degradation at NMJ. (C) Abs bind AChR and block acetylcholine from binding to receptor. [Image modified from Conti-Fine BM 2006 J Clin Invest (3).]

of autosensitization to AChR, where both thymic myoid cells and thymic epithial cells have been shown to express AChR (13). Recently, others have shown TLR4 and BAFF expression in the thymus of some patients with MG (14, 15). In addition to MG patients, those with systemic lupus erythematosus, rheumatoid arthritis, and rheumatic heart disease, among other autoimmune conditions, manifest thymic abnormalities (16). Since the thymus is a primary immune organ responsible for T cell development and selection, thymic abnormalities may alter the selection of the developing T cell repertoire. The contribution of T cells in the induction of MG will be discussed in the following sections.

MATURATION OF ANTI-ACHR ANTIBODY RESPONSES

There are five criteria that classify MG as an Ab-mediated autoimmune disease (3). First, patients with MG must have high-affinity Abs in their sera which are specific for self-antigens (auto-Abs). Second, auto-antibodies in MG patients such as anti-AChR or anti-MUSK have been shown to interact with AChR or MUSK and interfere with function of the NMJ. Third, passive transfer of Abs from MG patients into animals produces MG-like disease. Fourth, immunization of animals with target antigens, AChR or MUSK, causes MG-like disease. Finally, plasma exchange alleviates symptoms in MG patients.

The B cell receptor (BCR), immunoglobulin (Ig), is responsible for the specific recognition of antigens (Ag) (17). A mature B cell produces membrane bound Ig or secreted forms of Ig, Abs, that bind a specific antigen. Igs have characteristic Y shapes which are composed of two heavy and light chains. The two sides are identical and

consist of one heavy and light chain. Antigen specificity is a result of the interface between heavy and light chains in the arms of the Ab molecule (two antigen binding sites per molecule) (18). The tail of the Ab molecule consisting of the constant heavy chain is similar among Abs of similar class. There are five classes of Ig molecules (IgG, IgM, IgD, IgE and IgA). Each class of Ig has distinct effector functions and half-lives(19). Ab diversity during B cell development in the bone marrow is antigen independent and is the result of DNA rearrangements of both chromosomes in cells that express Ig genes (17). Ig diversity is continually created by activation of mature B cells in the periphery by recombination of multiple genes and the capability of the cell to alternate alleles to produce functional Igs (20).

Upon antigen activation of BCR in the periphery, a subtype of B cells, B2 cells, either remain in marginal zone and differentiate into short lived plasma cells (marginal zone B cells) that have germ-line encoded BCR or B cells migrate to primary follicles (follicular B cells), where interactions with follicular dendritic cells (FDCs) and T cells forms germinal centers (GCs) (Figure 2) (21). Due to somatic hypermutations (SH), antigen activated B cells acquire non-germ line point mutations at a rapid rate (0.3 mutations in variable region of Ig genes per cell division) for optimal recognition of antigens (22). When B cells receive appropriate signals from CD4+ T cells, Ig function is diversified further by class switch recombination (CSR), the somatic-recombination of heavy chain region of Ig genes (ie. IgM → IgG) (23). Therefore, CSR is termed a T-cell dependent antibody response. The GC formation coincides with various changes in B cells such as clonal expansion, BCR diversification by SH and CSR, and differentiation into long lived plasma cells or memory B cells (24, 25). The exact details of these GC

reactions are not clear. However, GC reactions are thought to regulate the selection of B cells that have Igs which have been mutated for optimal recognition of antigens.

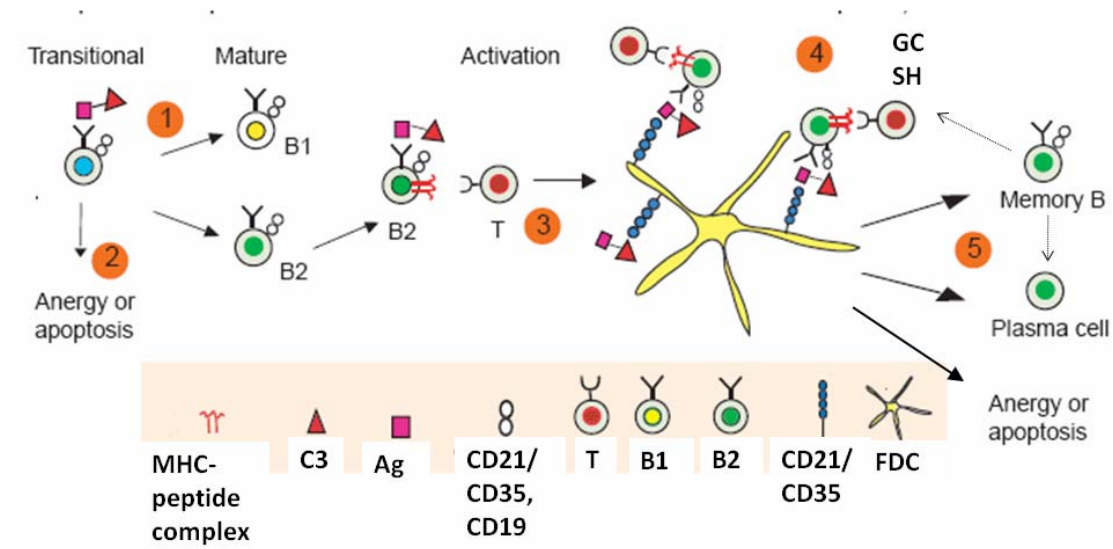

Figure 2: Current model of B lymphocyte differentiation. (1) Immature B cells leave the bone marrow and migrate into secondary lymphoid organs as transitional B cells. (2) Peripheral B cells that have high reactivity for self-antigen (Ag) are deleted by apoptosis or become anergic. B1 cells are self-replenishing cells with germ-line encoded Ig and are responsible for spontaneous secretion of natural Abs, while B2 cells after antigen encounter undergo a series of non-germ line point mutations and recombination of Ig genes. (3) Capture of Ag is mediated by the BCR complex which includes Ig, CD19, and CD21/CD35 (complement receptors). Ag complexed with C3 lowers the activation threshold of B cells. (4) Follicular dendritic cells (FDR) may phagocytize Ag but also capture immune complexes (Ab-C3-Ag) directly from B cells. Ag is taken up by FDCs or B cells and is rapidly processed and presented in association with MHC class I and II molecules to T cells, leading to the formation of germinal centers (GC). (5) B cells with high affinity for Ag either become antibody secreting plasma cells, memory cells, while B cells with low affinity for Ag undergo apoptosis or become anergic. [Image modified from Carroll MC 2004 Nat Rev Immunol (21).]

Multiple studies have shown that activated B cells, blasts, may undergo SH which is GC-independent and consequently prone to defects such as autoreactivity (26). This provides a mechanism to explain why even in healthy individuals an autoreactive mature B cell population exists. Extrafollicular SH Ig diversification may be crucial in protecting host from invasion by rapidly mutating microbes. One theory is that the host risks autoreactive SH to protect from death by infection (20). Others have suggested that a low level of self-recognition is beneficial and responsible for the activated phenotype of a particular subset of B cells that specialize in recognizing T-independent antigens; marginal zone B cells (MZB) (27). MZBs derive their name from where they reside in the spleen and are responsible for the earliest antibody responses during first infection with a particular microbe.

Pathogenic anti-AChR Abs are high affinity IgG1 which suggests B cell immune responses are T cell-dependent (28). IgG1 has the ability to induce receptor-mediated phagocytosis and cytotoxicity in other immune cells, and is capable of activating both the classical and alternative complement component systems (19). MG patients have higher serum levels of IL-18 and IL-12, most likely produced by CD4+ T cell, which support both CSR to IgG and activation of cytotoxic CD8+ T cells (29, 30). CD4+ T cells also boost B cell activity by secreting multiple cytokines such as IL-4 and IL-10 (3, 31). The role of CD4+ T cells will be discussed in more detail in Chapter 5. It is still unclear whether CD8+ T cells contribute significantly in the pathogenesis of MG (see Chapter 6).

EXPERIMENTAL AUTOIMMUNE MG

In mice, experimental autoimmune myasthenia gravis (EAMG), an MG-like disease is induced by immunization of C57BL/6 mice with *Torpedo californica* AChR (TAChR) emulsified in complete Freund's adjuvant (CFA) which contains heat killed *Mycobacterium* (32, 33). EAMG shares several characteristics in common with MG such as the presence of high-affinity anti-AChR in serum, IgG and complement deposits at NMJ, decrease in AChR at post-synaptic membrane, and destruction of the post-synaptic membrane folds, and an association of susceptibility with MHC allotype (34, 35). The main difference between EAMG and MG is the lack of thymic pathology in mice. The thymic pathology is not specific to patients with MG and has not been shown directly to trigger MG or EAMG in other animal models. We do not know whether thymic hyperplasia or thymomas are a cause or effect of MG due to AChR expression on thymic myoid cell. The pathogenesis of EAMG in mice models human MG closely and is considered an ideal model for immunotherapy development for antibody-mediated autoimmune diseases. Furthermore, mouse models have been critical to understanding the mechanisms in which tolerance is established.

THE ROLE OF INFECTION IN AUTOIMMUNITY

Many studies have indicated that microbes may be important for the development or enhancement of autoimmune responses (36). Autoimmune diseases are usually characterized by periods of severe symptoms, termed flares, which are followed by

periods of mild to absence of symptoms. These disease flares are often associated with infection (37). Several hypotheses regarding the role of infections in inducing or enhancing autoimmunity have been proposed (38, 39). Bystander activation of autoreactive cells may occur by the release of sequestered antigen from infected cells. Chemokines and cytokines produced during a particular immune response may also favor the survival and activation of autoreactive cells. Another possibility is that a microbial antigen may resemble a self antigen (molecular mimicry). AChR shares protein sequence homology with hundreds of microbial proteins from viruses or bacteria (ie. *E. coli*, *S. cerevisiae, V. cholerae, S. typhimurium*, Human Rotavirus, Herpes Simplex 1 virus, Vaccinia virus) (12, 40, 41). Post-infectious MG has been documented with chronic infections with HSV-1, Varicella-Zoster, HIV, and in patients with various suspected acute infections (42-46). The association between infection and MG is difficult to prove, since illness from infection precedes MG-like disease. This suggests that MG may result from multiple exposures to different pathogens and regulatory mechanisms such as peripheral tolerance and regulatory T cells may diminish with repeated pathogen exposures or with time. The mechanisms in which microbes alter peripheral tolerance in patients with MG or in animal models of EAMG needs to be investigated further.

Immunization of animals with CFA is thought to mimic an acute slow-growing infection, like *Mycobacteria* infection would cause (38). Conserved patterns from classes of pathogens such as bacteria, viruses, fungi and parasites are recognized by Toll-like receptors (TLRs) (47). Pathogen-specific motifs can be components of the surface of pathogens such as lipopolysaccharide (LPS) and peptidoglycan, or genomic components (DNA, RNA and dsRNA). *Mycobacterial* components such as CpG oligoneuclotides,

muramyl dipeptide, trehalos dimycolate, and lipoarabinomannans are all capable of being recognized by TLRs (48). TLRs non-specifically recognizing pathogens and stimulate the production of inflammatory cytokines (IL-1, IL-8, IL-6, and TNF-α) and interferons (48, 49). Inflammatory cytokines are important in the recruitment of leukocytes to the site of infection and the activation of phagocytes. Pro-inflammatory cytokine production induces activation of antigen presenting cells (dendritic cells, macrophages and B cells) by inducing CD80, CD86, CD40 and MHC I and II expression (37). Recently, animal models of SLE, a disease characterized by high affinity anti-dsDNA antibodies, showed that mice lacking TLR-9 form antibodies that do not class switch to isotypes capable of fixing complement, IgG2a and IgG2b (50, 51). Despite the potent CD4+ T cell activation in TLR deficient mice, antibody responses where diminished significantly. Immunization of animals with CFA and TAChR results in higher levels of circulating antibodies. Therefore, B cells may need TLR activation for normal function and also chronic stimulation may be the key to breaking B cell tolerance.

Recent studies of patients with MG indicate that innate immune responses may play an important role in disease development. MG patients have been reported to have an increased thymic expression of Toll-like receptor 4 (TLR4)(14). Some molecular mimics of AChR have been identified in microbes which produce LPS (for example *E. coli, V. cholerae, and S. typhimurium*) (39, 40). LPS induces the maturation of both macrophages and dendritic cells (DCs) and stimulates the production of IL-10, IFNγ, and BAFF, and other pro-inflammatory cytokines (47, 52, 53). Expression of BAFF, an essential B cell survival factor, which has been shown *in vitro* to induce CSR of both mouse and human B cells, is also increased in the thymus of MG patients (15, 54).

Therefore, we hypothesized that innate immune responses to AChR triggered by LPS would induce EAMG. Since the etiology of human MG is unknown, and possible microbial activation of immune responses might trigger autoimmunity, the development of a mouse model of MG triggered by innate immune responses is necessary.

OBJECTIVES OF THIS DISSERTATION

This dissertation aims to elucidate what signals are required for pathogenic Ab production in EAMG. To accomplish this goal a more direct and specific signal for B cell activation is the desired approach. Heat-killed desiccated *Mycobacterium* is complex having features that may alter B cell recognition such as the formation of denatured aggregated insoluble complexes of proteins. Studying specific TLRs signalling may be difficult when using whole bacteria since multiple ligands are present. The preceding discussion indicated that the B cell mitogen, LPS, may be implicated in the activation of autoeactive B cells. Highly purified LPS which has been tested to contain no agonist for other TLRs was used as an adjuvant in conjunction with AChR (LPS-AChR) to develop a new mouse model of MG (Chapter 3). A flow cytometry method was also developed to track AChR-specific B cells during the induction of EAMG (Chapter 4). We also investigated the contribution of CD4+ T cells and CD8+ T cells in the maturation of anti-AChR Ab responses in LPS-AChR induced EAMG (Chapter 5 and 6).

The proposed studies will increase our understanding of the mechanisms involved in the activation of autoreactive B and autoreactive T cells in EAMG. These aims evaluate AChR-specific B cells activation, survival, and function. Furthermore,

elucidating how LPS manages to break T and B cell tolerance will bring us closer to understanding potential conditions that lead to the development of MG and has broad applications to all autoimmune disease pathogenesis.

Chapter 2: Methods

INDUCTION OF EAMG

C57BL/6, CD4 -/- C57BL/6 and CD8 -/- C57BL/6 $CD4^{tm1Mak}$ mice were purchased from Jackson Laboratories (Bar Harbor, Maine, USA). AChR extracted from *Torpedoc californica* was purified on a neurotoxin affinity column, as previously described (33). EAMG was induced in anesthetized mice on day 0 by multiple s.c. injections in shoulders and foot pads with 20 μg AChR and 5 μg LPS in PBS (100 μl) emulsified in 100 μl IFA (LPS-AChR) or 20 μg AChR in PBS (100 μl) emulsified in 100 μl CFA (CFA-AChR). A separate group of mice were immunized with 100 μl of LPS (5 μg) emulsified in incomplete Freund's adjuvant (LPS) or 100 μl of PBS emulsified in CFA (CFA) for use as adjuvant controls. Both groups were anesthetized, and then immunized (200 μl/animal) with multiple s.c. injections in shoulders and foot pads. Mice were immunized with similar doses of AChR and respective adjuvant, on days 1, 28, and 56. All animals were housed in a barrier facility at the University of Texas Medical Branch and maintained according to the Institutional Animal Care and Use Committee guidelines.

MEASURING GRIP STRENGTH

Mice were exercised by 30 paw grips on the cage top grid. Following exercise, grip strength was measured by a dynamometer (Chatillon Digital Force Gauge, DFIS 2, Columbus Instruments). The maximal force (T-peak) applied to the dynamometer was

recorded, while pulling the mouse by its tail until release of paw grip from the grid. This measurement was repeated 5 times for each mouse. Grip strength ratio for each mouse at each time point was determined by dividing the average grip strength post immunization by the average grip strength prior to immunization. A ratio greater than 1 indicates a gain in grip strength and a ratio less than 1 indicates a loss of grip strength.

CLINICAL EVALUATION OF EAMG

Evaluation of disease severity and muscle weakness was performed immediately prior to blood draw and at 2 weeks after each immunization and measured as follows: **Grade 0,** normal mobility, posture and grip strength; **Grade 1,** hunchback posture, restricted mobility and decreased muscle grip strength after paw grip exercises; **Grade 2,** without exercise, observed hunchback posture, restricted mobility and decreased muscle grip strength; **Grade 3,** dehydrated and moribund with grade 2 weakness, death, or euthanasia due to paralysis**.**

CONJUGATION OF ALEXA FLUOR 647 TO ACHR

AChR was purified from *Torpedo californica* electric organs (Aquatic Research Consultants, CA) according to published method (33). AChR was concentrated by centrifugation with CentriconYM (10,000 molecular weight) centrifugal filters (Millipore, MA). AChR was then dialyzed in PBS by using Spectra/Por dialysis tubing

(12-14,000 molecular weight). AChR was labeled with Alexa Fluor 647 Protein Labeling Kit (Invitrogen) according to the manufacturer's instructions.

BLOOD COLLECTION AND ALEXA FLUOR 647-ACHR LABELING OF CELLS

Blood was collected from the tail vein into K2EDTA microtubes indicated times points post immunization. Blood was centrifuged at 500g for 15 min, and plasma removed for analysis of secreted anti-AChR Igs. Blood was then treated with BD Pharm Lyse Buffer. Fcγ receptors were blocked with anti- CD16/32 Ab (Ab 93, eBioscience). Fifty μl of whole blood was stained for surface markers with Alexa fluor 647 –AChR or Alexa fluor 647-Ovalbumin (Invitrogen) and PE-Cy7-anti B220 (RA3-6B2, eBioscience), then fixed and permeabilized by using a Cytoperm/Cytofix kit (BD Biosciences) according to standard protocols for flow cytometry. Cells were then stained with anti-IgG2b (R12-3, BD Biosciences) and anti-IgM (eB121-15F9, BD Biosciences) Abs or isotype controls. Cell populations were determined using a BD FACS Canto and FlowJo v 7.2 (Tree Star).

DETECTION OF IGM, IGG2, C3, AND MAC DEPOSITS AT THE NMJ BY IMMUNOFLUORESCENCE MICROSCOPY

Frozen sections (10 μm thick) were obtained from the tricep muscle and stored at -80°C. Slides were allowed to air dry and then were fixed in cold acetone. After being

washed with PBS, slides were incubated with Alexa Fluor 555-α bungarotoxin (1/100) (Invitrogen), and one of the following: Alexa Fluor 350 goat anti-mouse IgG2 (1/1000) (polyclonal, Invitrogen); rat anti-mouse C3 (1/50) (RmC11H9, Cedarlane Laboratories); or FITC rat anti-mouse IgM (1/500) (II/41; BD Pharmingen), overnight at 4ºC. Slides were washed with PBS. For C3 staining, Alexa Fluor 350 anti-rat IgG (1/100) was used as the secondary antibody (polyclonal, Invitrogen), and slides were incubated for 2 hr at RT. Sections were washed with PBS and viewed using a Olympus IX-70 microscope.

ELISA FOR ANTI-ACHR ANTIBODIES AND AVIDITY

Purified mouse muscle AChR (0.5 μg/ml) was coated on a 96-well microtiter plate (Dynatech Immulon 4 HBX; Dynatech Labs., Chantilly, VA) with 0.1 M of carbonate bicarbonate buffer (pH 9.6) overnight at 4°C. The avidity index (AI) was determined by modification of our anti-AChR antibody ELISA method (55). Plates were blocked for 30 min with 10% FBS in PBS and then washed. Sera were diluted 1:100 in PBS with .05% Tween 20 and incubated at 37ºC for 2 hrs. Plates were washed, then 2M, 1 M, 0.5 M of NaSCN, or PBS was added to dissociate low-avidity anti-AChR antibodies for 15 min at RT. Plates were washed and specific mouse isotypes were determined by HRPO conjugated anti-IgM, anti-IgG1, or anti-IgG2, diluted 1:1000 in PBS. Plates were incubated for 1hr at 37^{o}C. Finally, plates were washed and developed with ABTS Simple Solution (invitrogen). The absorbance at 405 nm was read. AI was calculated as follows: AI=(OD with NaSCN/OD without NaSCN).

FLOW CYTOMETRY OF LN CELLS

Lymph nodes were obtained from immunized mice on day 80. Following mechanical dissociation of lymph node cells, single-cell suspensions was made by using a 40-μm nylon cell strainer (BD Falcon). The following antibodies were used for flow cytometry analysis: APC-anti-mouse TCRβ (H57-597; eBioscience), PE-anti-mouse CD40L (MR1; eBioscience), FITC- anti-mouse CD8α (53-6.7; eBioscience), PE-anti-mouse CD4 (GK1.5; BD Pharmingen). Data were acquired on a FACS Canto (BD Biosciences) and analyzed using FlowJo v 7.2 software (Tree Star).

RADIOIMMUNOASSAY (RIA) FOR QUANTIFICATION OF ACHR IN MUSCLE

The total concentration of AChR per mouse carcass was determined according to a previously published method (33). Triton X-100 solubilized mouse muscle extracts were incubated with [^{125}I] α-bungarotoxin (BTX)-labeled (5×10^{-9} M), with and without benzoquinonium (10^{-3} M) and mixed with 10 μl of mouse anti-AChR serum. The resulting complex was precipitated by goat anti-mouse serum and then centrifuged. Radioactivity of the pellet was counted in a Packard gamma counter (Packard Instrument Co., Meriden, CT), and cpm values of samples with benzoquinonium were subtracted from cpm values of samples without benzoquinonium. The results were expressed as percentage of loss of [^{125}I]-labeled BTX- binding sites per gram of mouse carcass from immunized mice compared to naïve mice.

ELISA FOR BAFF

BAFF was measured using sandwich ELISA. Immulon 4 HBX plates were coated with 1.5 μg/ml anti-mouse BAFF (5A8; Alexis Biochemicals) in 0.1M carbonate buffer pH 9.5 overnight at 4^{o}C. Plates were washed with PBS supplemented with an additional 1% NaCl and 0.01% Tween 20. Plates were blocked with 2% BSA for 1hr at RT and then washed. Sera were diluted 1 to 50 in PBS 0.01% Tween 20. Next, 100 μl of diluted sera were incubated overnight at 4^{o}C. Plates were washed five times and then incubated for 1 hr at 37^{o}C with 1.5 μg/ml biotinylated anti-mouse-BAFF (1C9, Alexis Biochemicals) in PBS with .01% Tween 20. Plates were washed five times and then incubated for 30 min at 37^{o}C with streptavidin-HRP (1/250) in PBS with .01% Tween 20. Finally, plates were washed and developed with ABTS Simple Solution (Invitrogen), and absorbance was read at 405 nm.

Chapter 3: Bacterial Lipopolysaccharide Promotes Progression of EAMG

INTRODUCTION

Autoimmune diseases may be characterized by periods of severe symptoms, termed flares, which are followed by periods of mild or the absence of symptoms. These disease flares are often associated with infection(37, 43, 44, 56). Many studies have indicated that microbial infection may be important for the development or the exacerbation of autoimmune responses by triggering the production of inflammatory mediators such as IL-12, IFN-γ, IL-6, and TNF-α (31, 48, 49). Experimental autoimmune myasthenia gravis (EAMG), encephalomyelitis (EAE), thyroiditis (EAT), uveitis (EAU) are just a few animal models of autoimmune diseases that are induced by immunizing animals with an autoantigen emulsified in CFA, which contains heat- killed *Mycobacterium tuberculosis (38, 57).* Repeated immunization of mice with AChR emulsified in CFA induces EAMG, while repeated immunizations of AChR emulsified in incomplete Freund's adjuvant (CFA without *M. tuberculosis*) or with alum induces only mild disease or may actually induce tolerance (58-60). Therefore, the induction of EAMG is dependent upon the immunization with both AChR and heat- killed *M. tuberculosis.*

Another common adjuvant, LPS, a major component of the outer membrane of Gram-negative bacteria, was shown to induce or exacerbate the severity of disease in various models of autoimmunity, including experimental autoimmune arthritis, EAT, and SLE-prone MRL/lpr mice (56, 57, 61, 62). LPS is also known to induce strong inflammatory responses by activating the TLR4-MD2-CD14 receptor complex expressed by DCs and to a lesser extent on macrophages, endothelial cells, epithelial cells, and B

cells (14, 47). However, the role of LPS in MG induction has not been investigated. Of note, recent research in the mouse model of autoimmune Hashimoto's disease, EAT, suggests that the mechanism leading to disease in LPS-induced EAT is not the same as CFA-induced EAT (63). Since the etiology of human MG is unknown and the immune response triggered by different pathogens (or adjuvants) may be different, various mouse models for autoimmune disease is needed to understand the pathways that lead to autoimmune disease. In this chapter, we describe the development of a novel mouse model of EAMG using LPS in the place of desiccated *Mycobacterium* as an adjuvant.

RESULTS

LPS-AChR immunization induces EAMG in C57BL/6 mice like that seen following CFA-AChR immunization

To assess whether LPS can induce EAMG, male C57BL/6 mice, 8 weeks old, were randomly divided into five groups (n-5-8 per group). A group of mice remained untreated throughout the experiment (naïve). EAMG was induced by immunizing mice subcutaneously with AChR (20 μg) emulsified with either CFA or IFA and LPS (5 μg). Since the effect of LPS immunization alone is unknown in this model, a group of mice were immunized subcutaneously with PBS emulsified in IFA and LPS (5 μg) or CFA. Mice were immunized a second time on day 30 in a similar manner. The first clinical sign of EAMG in mice is a loss in muscle strength in upper limb muscles after exertion by paw grip exercises. The kinetics of variations in muscle strength was evaluated by determining the grip strength ratio after exercise for each mouse. A ratio > 1 indicates an

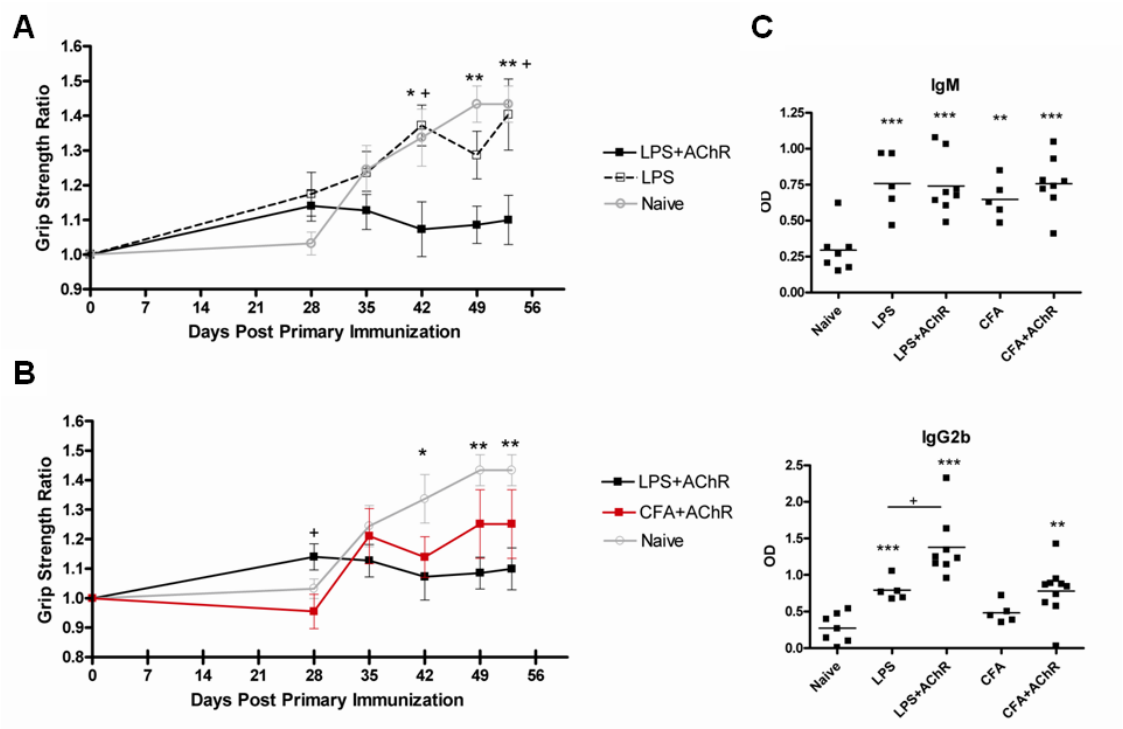

Figure 3: Grip strength ratio kinetics and sera anti-AChR Ab titers. (A) Kinetic of grip strength ratio at indicated time points for naïve, LPS-AChR and LPS immunized mice or (B) naïve, LPS-AChR and CFA-AChR immunized mice. Square indicates mean grip strength ratio for indicated group at that specific time point. Error bar indicates SEM. A Student's t-test was used to compare mean grip strength ratio of LPS-AChR (A) or CFA-AChR(B) immunized to naïve mice * p<.05, ** p<.01, while + p<.05 indicates differences between LPS-AChR and LPS (A) or CFA-AChR (B) immunized mice. (C) Anti-AChR IgM and IgG2 were measured at day 42 by ELISA. Square indicates OD value for each individual mouse. Bar indicates mean OD value (n=5-8, t-test, * p<.05, ** p<.01, ***p<.001 compared to naïve, + p<.05 compared to LPS immunized mice. Experiment is representative of three independent experiments.

increase in limb strength, and a ratio < 1 indicates a loss of grip strength. LPS-AChR immunized mice had significantly lower average grip strength ratio compared to LPS immunized and naïve mice by day 42 post primary immunization (Figure 3A). However, there was no significant difference in the average grip strength ratio between LPS-AChR and CFA-AChR immunized mice (Figure 3B). These data indicate that LPS-AChR immunization may induce clinical signs of EAMG.

In order to establish that the loss in limb strength may be due to the induction of anti-AChR Abs, we measured sera anti-AChR Abs by ELISA at day 42, the time of onset of muscle weakness (Figure 3C). All immunized mice had significantly elevated sera anti-AChR IgM compared to naïve mice. Both LPS and LPS-AChR immunized mice produced statistically significant amounts of anti-AChR IgM and IgG2b. Of note, CFA immunization of mice did not induce anti-AChR IgG2b secretion but induced the production of anti-AChR IgM. While CFA-AChR immunization of mice induced production of both anti-AChR IgM and IgG2. These results indicate that immunization with CFA requires the addition of AChR for CSR of IgM to IgG2 while LPS does not. However, the addition of AChR in the LPS immunized mice had significantly enhanced the production of anti-AChR IgG2 (Figure 3C).

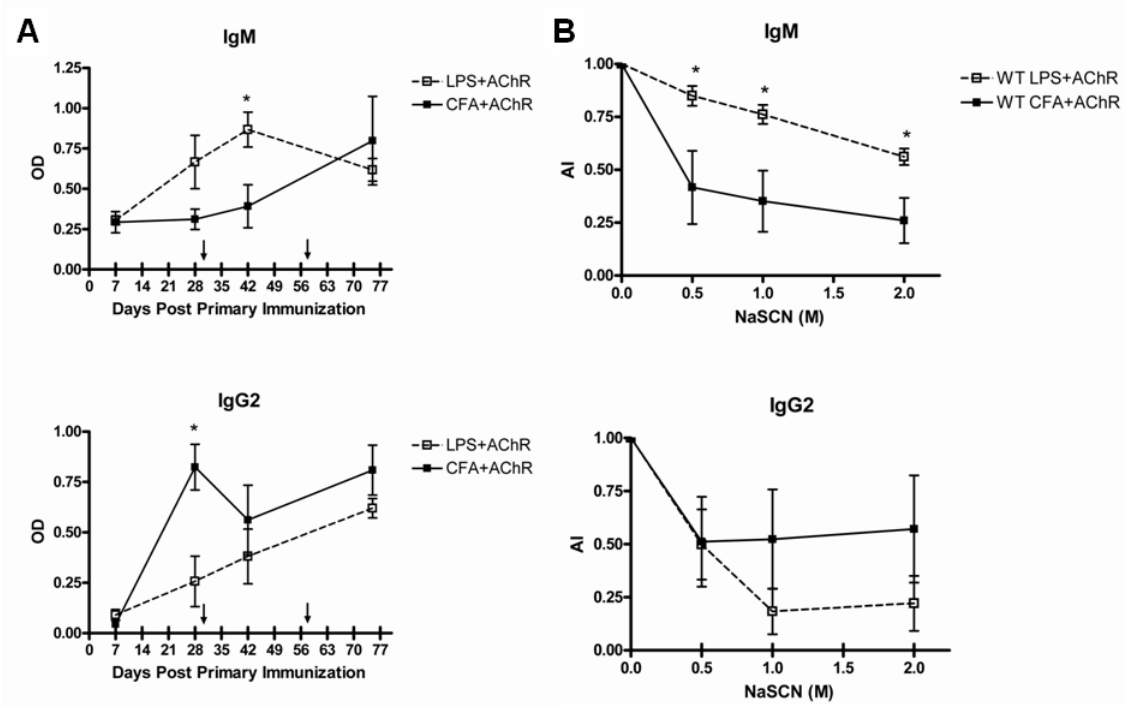

Figure 4: Comparison of kinetics and avidity of anti-AChR Abs between CFA-AChR and LPS-AChR immunized mice. (A) Sera anti-AChR IgM and IgG2 concentrations were determines at various time points post primary immunization. Anti-AChR Ab response is shown as mean OD with SEM (n= 5-10) (B) Mean avididty index (AI) of anti-AChR IgM and IgG2 at onset of EAMG, day 42. Statistical significance (* $p<.05$) was determined by a Student's t-test comparing data from LPS-AChR to CFA-AChR immunized mice. Arrows indicate time of boost immunization. Experiment was repeated with similar results.

To further characterize the Abs produced by mice which develop EAMG, we next analyzed the kinetics of anti-AChR AB production and the avidity of AChR-specific Abs (Figure 4). LPS-AChR immunized mice had elevated levels of anti-AChR IgM at days 28 and 42 compared to mice immunized with CFA-AChR (Figure 4A). In addition to the elevated quantity of anti-AChR IgM produced by LPS-AChR immunized mice, the avidity of the anti-AChR IgM was statistically stronger for mouse AChR than the IgM produced by CFA-AChR immunized mice (Figure 4B). There were no significant differences between the avidity of anti-AChR IgG2 between LPS-AChR and CFA-AChR immunized mice. CFA-AChR immunization led to earlier production of anti-AChR IgG2 than LPS-AChR immunization. These data further demonstrate a difference in the quantity and quality of anti-AChR Abs induced by the adjuvants LPS and CFA.

LPS-AChR immunization of mice leads to significant reduction of muscle AChR and the deposition of Immune complexes at the NMJ

To determine whether anti-AChR Abs cause a loss of muscle AChR, we used a radioimmunoassay (RIA) to quantify α-bungarotoxin (Btx) binding sites in the muscles of LPS-AChR-immunized mice. Btx, a component of the venom from the *Bungarus multicinctus* snake, binds specifically to muscle AChR. The percentage of loss of Btx-binding sites was determined by comparing AChR content from immunized to that from naïve mice (Figure 5). LPS-AChR- immunized mice [mean 31.24 ± 13.07% (n=5)] have an average of 9% greater loss of functional AChR than do CFA-AChR-immunized mice [mean 22.17 ± 11.31% (n=5)]. There were no significant differences in AChR loss

between CFA-AChR and LPS-AChR immunized mice (t-test, p= 0.6). These results confirm that there is a loss of functional muscle AChR following LPS-AChR immunization.

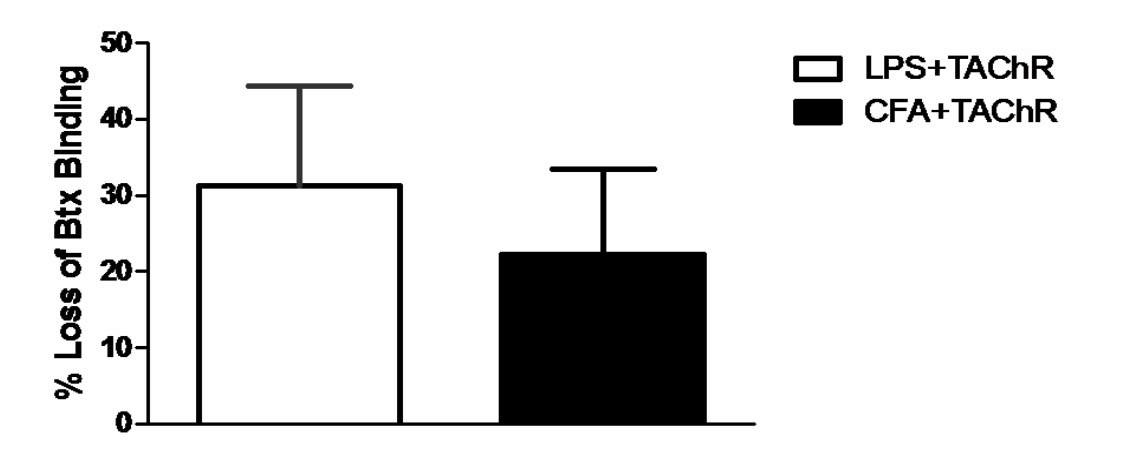

Figure 5: LPS-AChR immunization of mice leads to loss of functional muscle AChR. Mouse muscle extracts were analyzed by RIA for AChR content. EAMG was induced in C57BL/6 mice by multiple immunizations. Mean percentage of AChR loss compared to naïve mice for LPS-AChR or CFA-AChR immunized mice.

AChR loss in MG and EAMG is mediated by IgG and complement deposits at the motor end plate. Frozen limb muscle sections obtained from mice at four weeks post boost immunization with LPS-AChR were double stained with Btx to locate AChR at the NMJ and with anti-IgG, anti-C3, or anti-C5b-C9 (MAC) to determine the location of immune deposits in limb muscles (Figure 6). Pathogenic IgG, C3, and MAC deposits co-localized to the NMJ following LPS-AChR immunization, which suggested that IgG could bind AChR and activate complement at the motor endplate. Similar results were

previously reported by others for immunization with CFA-AChR (we confirmed these results in Chapter 5).

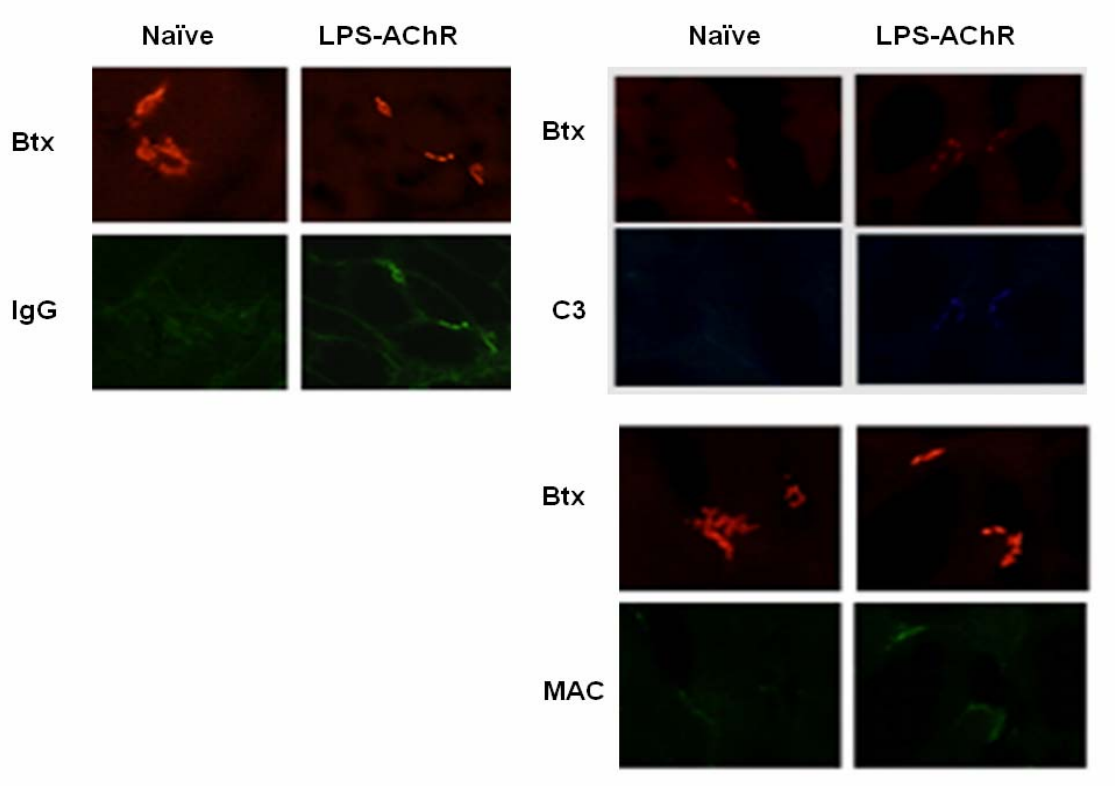

Figure 6: Antibodies mediate muscle weakness of LPS-AChR immunized mice. EAMG was induced in C57BL/6 mice by multiple immunizations with AChR in IFA and LPS. Cryostat sections of right tricep mucle were stained with α-bungarotoxin (Btx) (red) to identify NMJ and anti-IgG (green), anti-C3 (blue), or anti-c5b-9 (MAC). Data shown are representative of sections obtained from several mice from each group (n=5). 200 X magnification.

To determine whether mice with EAMG have altered TLR4 expression, we measured the percentage of TLR4 expressing peripheral blood mononuclear cells (PBMCs) by flow cytometry on day 42, when signs of EAMG were first observed (Figure 7). The percentage of TLR4+ MHC class II (I-A/I-E) expressing cells was compared across all treatment groups. CFA-AChR and LPS-AChR immunization led to a 3-fold and 2-fold increase respectively, in the frequency of circulating TLR4+ antigen presenting cells (I-A/I-E+) compared to naïve and CFA immunized mice. Immunization with LPS alone induced TLR4 expressing cells at higher frequencies that LPS-AChR immunized and naïve mice.

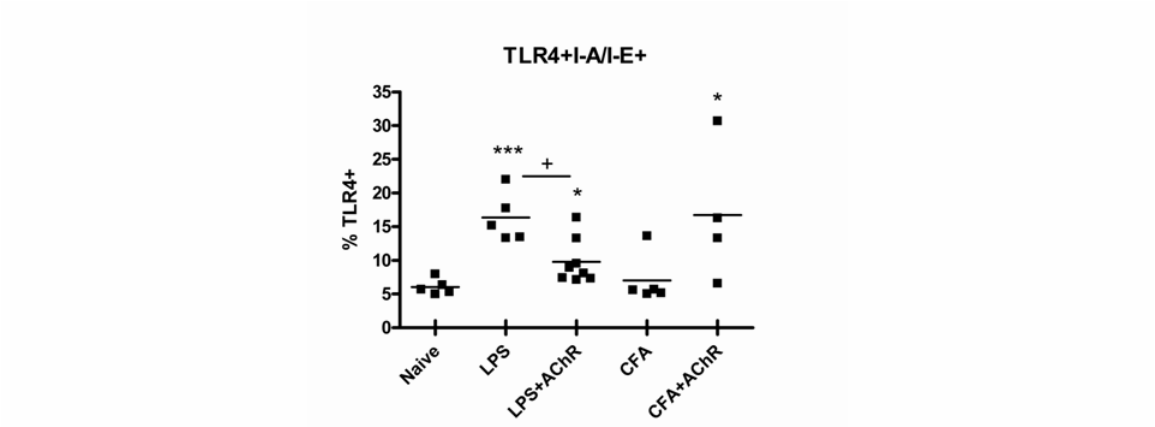

Figure 7: TLR4 expression by I-A/I-E+ PBMCS. Mice were treated as indicated on the x-axis by two immunizations, 30 days apart. Peripheral blood cells were stained with anti-I-A/I-E and anti-TLR4. Each square represents the percentage of live TLR4+ cells which express I-A/I-E in blood of individual mouse. The bar indicates the mean percentage (n=5-8, * p<.05, *** p<.001, t-test between immunized and naïve, + p<.05, t-test between LPS and LPS-AChR immunized mice.

DISCUSSION

In this chapter we describe the development of a new model for myasthenia gravis using the T-independent mitogen, LPS, in place of desiccated *Mycobacterium* as an adjuvant for immunization with AChR in incomplete Freund's adjuvant. Mice developed MG-like disease after boosting at day 28. Muscle weakness was associated with the production of pathogenic complement-binding anti-AChR IgG2 in blood, deposits of IgG, C3, and MAC at the NMJ, and a greater than 30% loss of muscle AChR. MG-like disease and pathology in LPS-AChR EAMG were comparable to those found with CFA-AChR induced EAMG. Taken together, these data demonstrate that LPS can be used as an adjuvant to induce EAMG.

Of interest, mice immunized with LPS alone produce low levels of anti-AChR IgG2 but do not develop signs of EAMG. One possible explanation is that the quantity of anti-AChR IgG2 may not be sufficient to induce EAMG. However, it may also indicate that other factors may be involved in the pathogenesis of LPS-AChR induced EAMG. The presence of protein Ag, such as AChR, is known to elicit the activation of T cells. The role of CD4+ T cells and CD8+ T cells in this new model of EAMG will be described in Chapter 5 and 6, respectively..

Recently, others have shown that thymic TLR4, CD14 and MD2 expression is increased on DCs and thymic epithelial cells (TECs) of MG with thymic hyperplasia and to a lesser extent with thymic involution but not thymoma (14). LPS mimics infection by triggering innate immune responses through the activation of TLR4-MD2-CD14 receptor complex (64). TECs and DCs secrete the inflammatory cytokines, TNF-α and IL6, when

stimulated with LPS (65). The thymus is implicated in the pathogenesis of MG for several reasons. First, thymic pathology (involusion, hyperplasia, and thymoma) occur in a majority of MG cases (16). Second, both thymic myoid cells and TECs have been shown to express AChR (66, 67). Third, AChR-specific B cells have been identified in the thymus of MG patients. Finally, the thymus is a primary immune organ responsible for T cell development and selection; thymic infection may be important in the development of autoimmune disease by inducing thymitis or thymic hyperplasia and interfering with the selection of the developing T cell repertoire (68).

Since EAMG does not induce thymic pathology, we measured the expression of TLR4 on circulating PBMCs. The frequency of TLR4+ cells was significantly higher than naive mice in mice immunized with LPS, LPS-AChR or CFA-AChR but not with CFA. Of note, CFA immunization of mice was also the only immunization group that did not induce anti-AChR IgG2 production. These data indicate that TLR4 signaling may be important for the CSR of IgM to IgG2.

In conclusion, this is the first report of an LPS-AChR induced model of EAMG. Immunization of mice with LPS alone enhances the expression of TLR4 and the production of anti-AChR IgG2 Abs, whereas immunization with CFA requires the presence of AChR to induce similar levels of TLR4 and IgG2b. These data suggests that the two models of EAMG, LPS-AChR induced and CFA-AChR induced, promote different immune mechanisms that trigger autoimmunity (Chapter 5 and 6).

Chapter 4: The Characterization of AChR-Specific B Cells by Flow Cytometry

INTRODUCTION

MG is diagnosed by radioimmunoassay, ELISA or ELISPOT-based detection of sera anti-AChR Igs (3, 74, 75). However, the anti-AChR Ig titer alone is not a reliable predictor of disease severity (76, 77).

Since B cells express both surface and/or secreted forms of Igs, which are capable of recognizing AChR, measuring antibody secretion alone is an indirect and limited means of determining B cell activation. We developed a new diagnostic and potential biomarker flow cytometry assay for MG which identifies AChR-binding B cells. We used Alexa fluor-conjugated AChR as a probe for identifying potentially pathogenic peripheral blood B cells from mice with EAMG. Similar techniques have been used to study protective antigen-specific B cells responses towards tetanus toxin, rotavirus, influenza and autoreactive specific B cell responses in diseases such as SLE and pemphigus vulgaris (78-81). But in these studies the significance of antigen-specific B cell frequencies was never evaluated directly for protection from infection or for induction of pathogenic autoimmune B cell responses. In this study, we demonstrate, for the first time, the frequency of a subset of AChR-binding B cells which express IgG2b in the peripheral blood at the onset of EAMG, and that the population size of these AChR binding B cells also correlates with clinical markers of disease severity.

RESULTS

Detection by flow cytometry of AChR-binding B cells among PBMCs of mice with EAMG

Given the pathological significance of complement activation in MG, we conducted a comparative flow cytometry study of AChR-binding B cells which express IgM or IgG2 in mice (82). To activate AChR-specific B lymphocytes, we immunized mice multiple times with AChR in CFA. The protocol was optimized by using whole blood drawn from mice with EAMG approximately 2 weeks following the third immunization with AChR emulsified in CFA; these results were then compared to LPS-immunized mice. Alexa fluor 647-AChR was used as a probe for potentially autoreactive AChR-specific B cells, while staining with Alexa fluor 647-OVA was used as an antigen specific negative control. Shown in Figure 8 is the typical staining patterns observed from blood stained with Alexa fluor -AChR, anti-B220, anti-IgM, and anti-IgG2. Alexa fluor-AChR preferentially bound to B220-expressing cells, which indicated to us that B cells are the main subset of peripheral lymphocytes capable of binding AChR (Figure 8A). Furthermore, B220+ AChR-binding lymphocytes are most prominent in

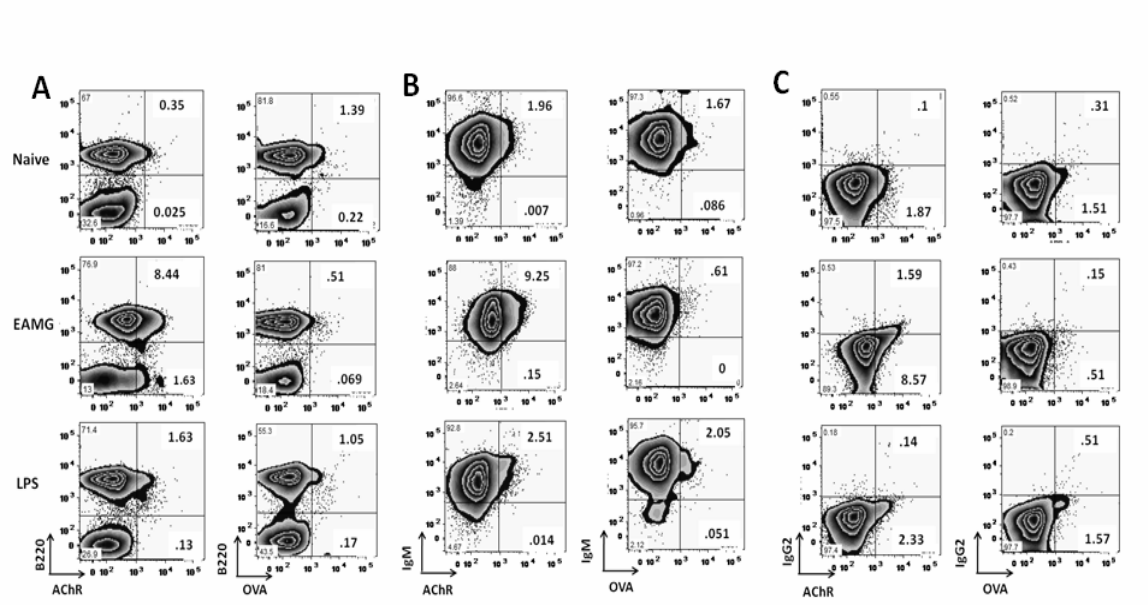

Figure 8: The characterization of AChR-binding peripheral blood lymphocytes by flow cytometry. Representative flow cytometry analysis of peripheral blood lymphocytes from naïve, LPS-immunized or CFA+AChR-immunized (EAMG) mice, 75 to 80 days post primary immunization. Cells were first gated on lymphocytes and then analyzed for B220 expression and either AChR binding or OVAbinding (A). Then lymphocytes were gated on B220+ cells to characterize IgM (B) or IgG2 (C) expression and either AChR binding or OVA binding. The numbers shown in bi-exponential plots indicate the relative percentage of cells in each quadrant. The experiment was repeated 5 times with similar results.

mice with EAMG. There is no significant increase in B220+ OVA-binding lymphocytes in mice with EAMG. These data suggest that the expansion of B220+ lymphocytes in mice with EAMG is specific to AChR-binding cells. To characterize these cells further, lymphocytes from the upper quadrants (B220+) were gated on and evaluated for expression of IgM or IgG2 and AChR-binding (Figure 8B&C). Although all mice had B220+IgM+ AChR-binding cells, these cells appeared at the highest frequencies in mice with EAMG (Figure 8B). Conversely, only mice with EAMG had elevated frequencies of

B220+IgG2+ AChR-binding cells (Figure 8C). Background staining of blood lymphocytes with Alexa-OVA provided results showing the AChR-binding B cells are responsible for the increase in B cell frequencies. To confirm the specificity of this assay, inhibition of Alexa fluor 647-AChR binding to B cells was shown by incubating the cells with a 10-fold excess of unlabeled AChR prior to fluorescent labeling (Figure 9). Alexa fluor-AChR staining of total B220+ cells, and IgM+ and IgG2+ B cells was significantly reduced by inhibition with unlabeled AChR.

To determine the significance of the differences observed for AChR-binding B cell frequencies between mice with EAMG and controls, we evaluated AChR-binding B cell frequency at different time points following immunization with AChR in CFA. (Figure 10). Using the analysis scheme described in Figure 8, we found no significant differences in AChR-binding B cell frequencies a week following the primary AChR immunization. After the second AChR immunization, the frequencies of AChR-binding peripheral blood B cells began to rise. Both B220+IgG2+ and B220+IgM+ AChR-binding B cell frequencies were significantly elevated compared to healthy and LPS immunized mice. After the third immunization, all subsets (B220+, B220+ IgM+, B220+IgG2+) of AChR-binding B cells analyzed were significantly elevated compared to findings with subsets in healthy naïve or LPS immunized mice (Figure 10).

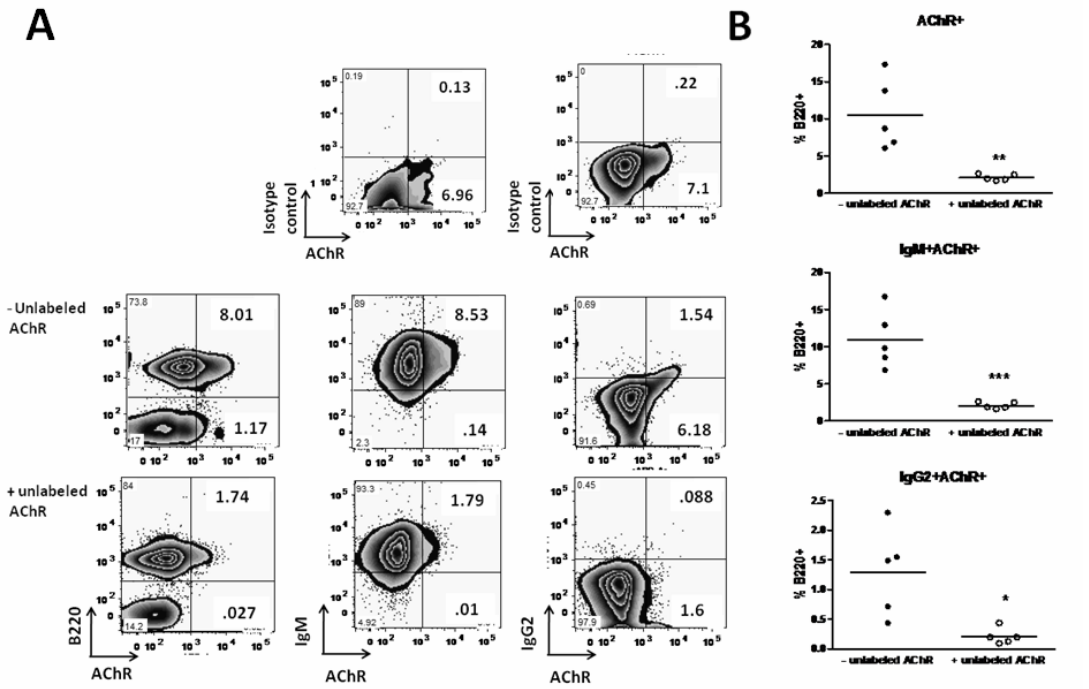

FIGURE 9: Inhibition of Alexa fluor-AChR-binding to peripheral blood B cells with unlabeled AChR. Representative flow cytometry staining of peripheral blood lymphocytes with (+) or without (-) blocking by incubating cells with (+) unlabeled AChR prior to staining with Alexa fluor-AChR; anti-B220 and anti-IgM, anti-IgG2, or isotype controls (A). The numbers shown in bi-exponential plots indicate the relative percentage of cells in each quadrant. The mean percentage of B-cell, AChR-binding subsets with (+) or without (-) blocking with unlabeled AChR (B). Each circle represents the frequency of AChR-binding B cells after 3 immunizations with CFA+AChR from individual mice having EAMG (n=5).The bar indicates the mean frequency of AChR-binding B cells. The data shown are from one experiment that was repeated three times. *P<.05, **P<.01, ***P<.001. t-test.

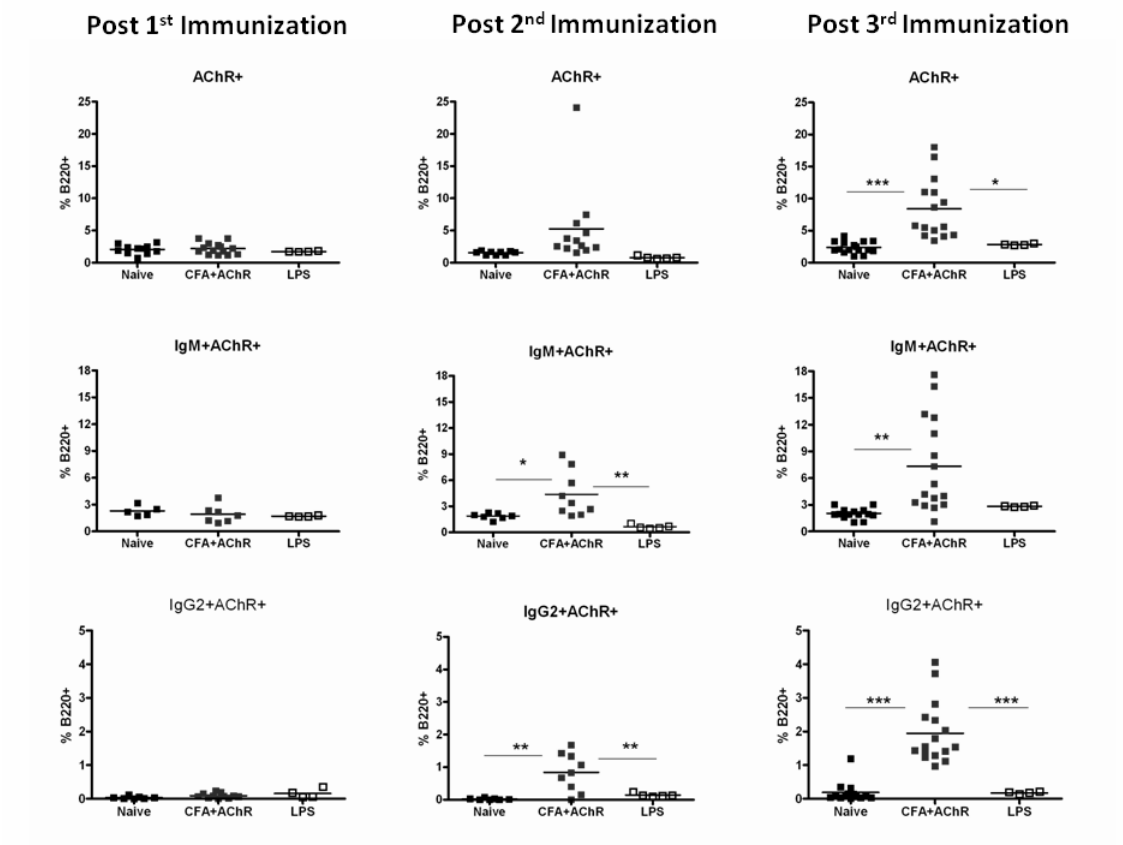

FIGURE 10: The kinetics on the frequencies of AChR-binding B cells . Shown is the mean percentage of subsets of peripheral blood B cells which are AChR-binding from naïve, LPS- immunized or CFA+AChR-immunized (EAMG) mice. Cells were analyzed as shown in Fig. 1. Each square represents the frequency of the total AChR-binding B cells (top row), AChR-binding IgM+ B cells (middle row) or AChR-binding IgG2+ B cells (bottom row) from individual mice with EAMG after each immunization. Significant differences between populations were determined by ANOVA with Tukey's post hoc test and represented by a * $P<0.05$, ** $P<0.01$, and *** $P<0.001$. Results shown are combined from multiple flow cytometry experiments with a total n=5-15 mice per group.

The appearance and frequency of peripheral blood AChR-specific B cells correlates with the severity of EAMG

Although the presence of serum antibodies to AChR indicates a possible diagnosis of MG, anti-AChR Ig concentrations are not a reliable markers for disease severity (10). Clinical parameters of EAMG severity were used to determine whether the frequencies of peripheral blood AChR-specific B cells correlate with disease severity. The clinical grade of EAMG is a combination of several observed parameters of EAMG, such as posture,mobility, and muscle strength. Healthy unimmunized mice were assigned a clinical score of 0. A score of 1 is associated with no signs of EAMG prior to exercise or mild disease, a 2 indicates overall moderate symptoms of limb weakness, a score of 3 is associated with significant signs of muscle weakness without exercise and severe disease. After mice were immunized three times (day 75) with AChR in CFA, the frequencies of peripheral blood AChR-specific IgM + and IgG2+ B cells were compared with the clinical grade of disease (Figure 11). Earlier time points (days 7, 28, 42) were not evaluated due to the lack of animals with severe disease. IgM+ AChR-specific B cells in blood had a significant correlation with the clinical grade of EAMG ($r = 0.6638$, $p<.0001$, n=5-7 per grade) (Figure 11A). IgG2b+ AChR -specific B cells in blood also had a strong correlation with clinical grade ($r = 0.767$, $p<.0001$, n=5-7 per grade) (Figure 11C).

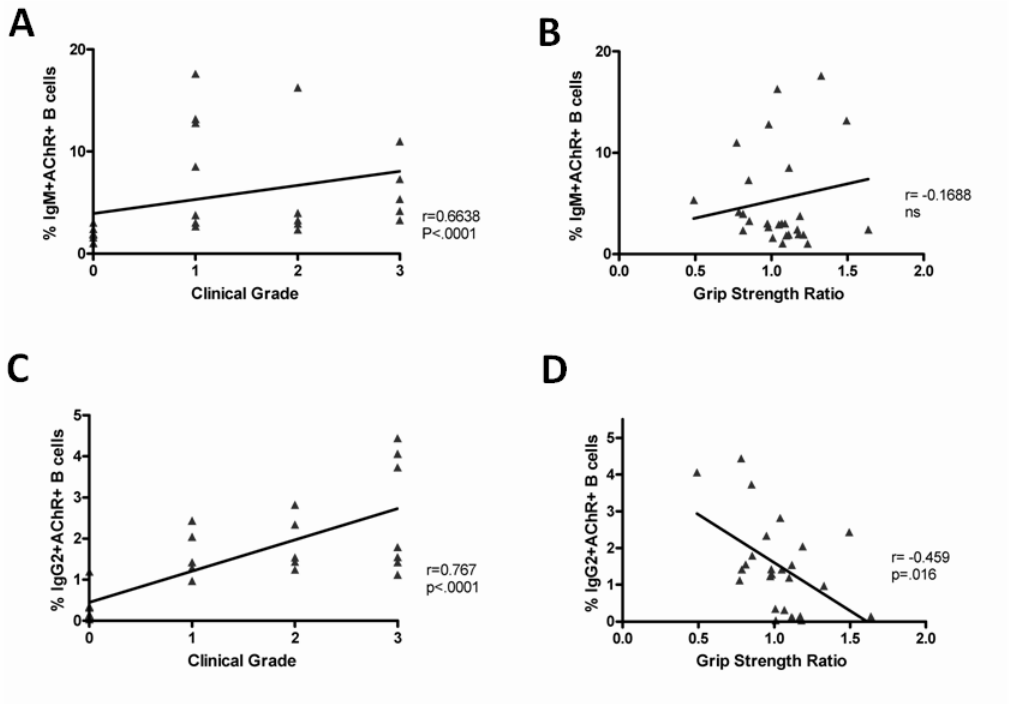

FIGURE 11: Correlation between AChR-binding peripheral blood B cells and markers of disease severity. Each triangle represents the frequency of AChR-binding IgM + (A&B) or IgG2+ (C&D) after 3 immunizations with CFA+AChR from individual mice with EAMG (clinical grades 1-3) and naïve mice (clinical grade 0) (n=5-7 per group). Clinical evaluation was completed at the time of blood draw (day 80). R is the Spearman coefficient between AChR-binding B-cell frequency and clinical grade (A&C) or grip strength loss represented by the grip strength ratio (B&D).

Grip strength ratios are a more objective measurement of loss of muscle strength, described in detail in methods. A grip strength ratio >1 indicates an increase in strength over time, while a grip strength ratio $\leq$1 indicates a loss of grip strength overtime. Mice which developed severe EAMG would have grip strength ratios $\leq$1. IgM+ AChR binding B cells in blood had a no significant correlation (r = -.1688, p=.3978, n= 26) with grip strength ratio (Figure 11B). However, IgG2b+ AChR-binding B cells in blood had a

negative correlation ($r = -.459$, $p<.016$, $n=26$) with the grip strength ratio (Figure 11D). Taken together, these results indicate that increased frequencies of peripheral blood AChR-specific B cells correspond to loss of limb muscle strength (grip strength ratio <1) and to higher clinical grades of disease. Furthermore, AChR-specific IgG2 B cell frequency is a good biomarker of disease severity.

Plasma secreted anti-AChR Igs do not correlate with the AChR-specific B cell frequencies in mice with EAMG

It has been previously demonstrated that sera or plasma anti-AChR Igs titers alone is not a reliable predictor of disease severity. However, this new assay demonstrated that the frequencies of AChR-specific B cells is useful biomarker for disease severity. We also evaluated the association between AChR-specific, B-cell frequencies and plasma anti-AChR concentrations (Figure 12). Mice were immunized with CFA and AChR and bled at days 7, 28, 42, and 56. Plasma was separated from cells by centrifugation and analyzed for secreted anti-AChR Igs. Blood was then stained for AChR-binding B cells. Overall, the concentrations of anti-AChR Igs and frequencies of AChR-specific B cells tended to increase throughout the induction phase of EAMG (Figure 12A&C). However, at a time when animals have no disease symptoms (day 28), plasma anti-AChR IgG2 titers are significantly elevated. After boost immunization (day 42), mice began to show signs of disease, while plasma anti-AChR IgG2 titers started to decrease, the AChR-specific, IgG2-expressing B cells first began to appear in the peripheral blood. No significant correlation was found between individual mouse plasma anti-AChR level and specific peripheral B cell populations (Figure 12B&D).

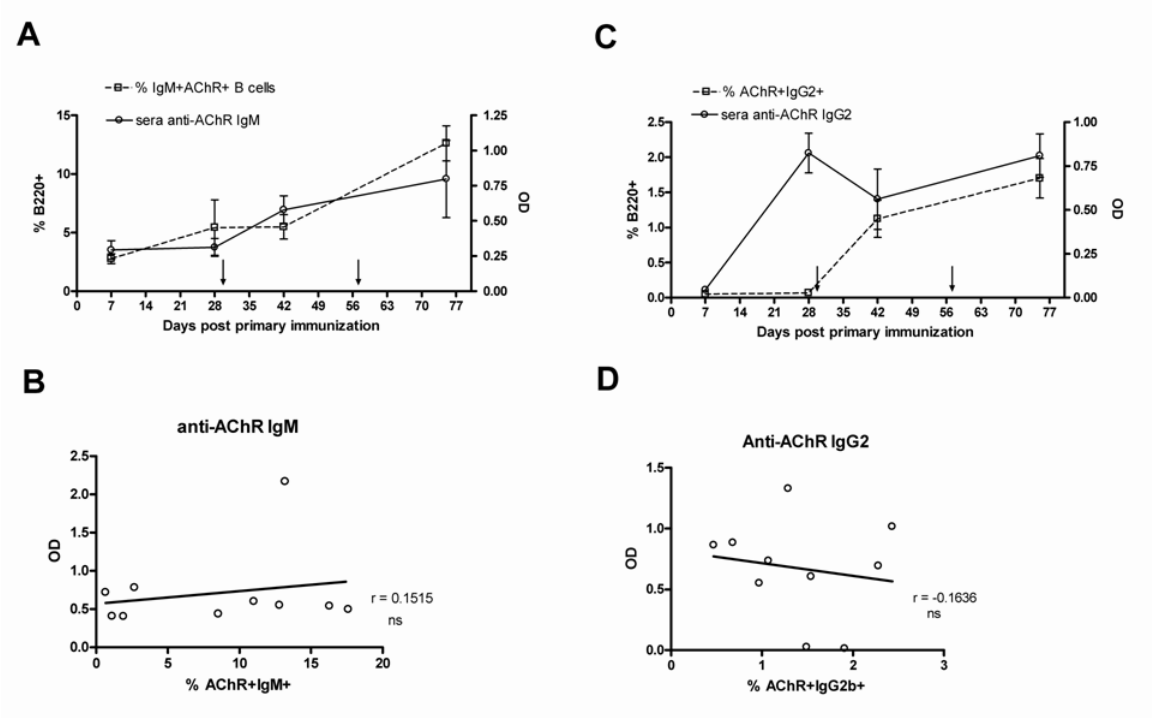

FIGURE 12: Concentration of sera anti-AChR Igs does not correlate with the AChR-specific B-cell. Mean IgM (A) and IgG2 (C) expressing AChR-specific B-cell frequencies are shown by open squares with a broken line with SEM, and values are indicated on the left y-axis. Mean and SEM plasma anti-AChR IgM (A) and IgG2 (C) OD values determined by ELISA are shown by open circles with a solid line, and values are indicated on right axis. Spearman correlation between individual plasma anti-AChR IgM (B) or IgG2 (D) concentrations and the frequency of the AChR-binding B cells after day 42 post immunization. Black arrows indicate time of boost immunizations. Results shown are from one experiment with a total n=4-10 mice. Experiment was repeated with similar results. r, Spearman correlation coefficient; ns, not significant.

DISCUSSION

Our data demonstrates that Alexa fluor-AChR conjugates could be used to identify and characterize subsets of B cells with specificity for AChR. The vast majority of cells which bound AChR express a B cell phenotype, B220+IgM+ or B220+IgG2+. On average less than 1% of Alexa fluor-AChR-binding cells were B220- but CD3+ (data not shown), the significance of this population was not investigated further due to small population frequencies, instead we focused our attention on B220+ AChR-binding cells. Our data suggests that B220+IgM AChR-binding B cells are part of the B cell repertoire in C57/BL6 mice, since these cells were detected in naïve, LPS stimulated and EAMG mice. However, frequencies of B220+IgM+ AChR-binding cells were significantly elevated in peripheral blood of mice with EAMG. We found that the frequency of B220+IgG2+ AChR-binding cells is a better indicator of disease than B220+IgM+ cells. Since naïve or immature B cells are IgM+, it is likely that these IgG2+ cells are AChR-experienced B cells subsets such as activated blasts, memory, or terminally differentiated plasma cells. Thus, IgG2+ AChR-binding B cells are a marker for EAMG and its frequency correlates with multiple parameters of disease severity. This data is in agreement with previous reports of B cell Ig isotypes in patients with MG indicating that at onset of disease there appears to be a conversion of IgM to IgG AChR specific cells.

Currently, diagnosis of MG involves a combination of clinical history, nerve stimulation tests, and blood test for serum Abs against AChR (71). An interesting observation in this study is that the frequency of peripheral blood AChR-binding B cells does not correlate with the concentration of anti-AChR Igs. These results are consistent with those in previous studies of peripheral blood antigen-specific B cells against infection (79, 83). These data suggest that the expansion of AChR-specific B cells observed in the blood of EAMG mice is not due solely to the presence of anti-AChR-secreting B cells, but that these cells are there in addition to memory B cell or activated blast cells. To our knowledge, no studies have been done that have characterized the relationship between autoantibody secretion and peripheral blood antigen-specific autoreactive B cells detected by flow cytometry in non-genetically manipulated mice, such as those shown here. However, it has been reported that virus-specific, antibody-secreting B cells in lymph nodes in mice post infection are comprised of a smaller subset of the total virus-specific cells identified by flow cytometry.

More importantly, these data support the theory that B cells may contribute to the pathogenesis of EAMG by a means other than that of antibody secretion. Studies in μMT mice indicated that B cells are essential for inducing EAMG and are also important for actvating T cells (84, 85). The deposition of anti-AChR Abs in muscle is capable of destroying the NMJ by activation of the complement component system, which causes inflammation (86). Activated B cells can produce cytokines, such as IL4, IL-10, TNF-α, IFN-γ, and IL-6, which can activate dendritic cells (DCs) and other mononucleated cells, skew immune responses, and cause inflammation (87). B cells

are also capable of antigen presentation and, therefore, have the ability to activate autoreactive CD4+ T cells (21, 59).

We have developed a simple assay for detecting by flow cytometry peripheral blood AChR-specific B cells. This assay uses no radioactivity and can screen blood samples in slightly more than one hour for increased frequency of AChR-specific B cells. The characterization of pathogenic AChR-specific B cells will be a valuable tool for understanding autoantibody-mediated disease pathogenesis as well. The use of flow cytometry will enable us discern more information about the types of cells producing anti-AChR antibodies, such as Ig class, frequency, activation, cell signaling, and cytokines. Furthermore, detection of AChR-specific B cells could be useful, not only for the rapid diagnosis of MG, but also as a biomarker for disease activity.

Chapter 5: The Effect of CD4 Deficiency on Anti-AChR Ig Responses in LPS-AChR Induced EAMG

INTRODUCTION

Previously, it has been demonstrated that CFA-AChR immunization requires CD4+ T cells for the induction of EAMG. CD4 -/- mice, as well as MHCII -/- mice are resistant to the development of CFA-AChR induced EAMG (88-90). In addition, studies involving blockade of costimualtory signals, such as CD86, CD28, CD80, and CD40L, have affirmed that T cell stimulation is critical for development of CFA-AChR induced EAMG (91, 92). Previously, we have shown that immunization of mice with AChR emulsified in IFA with LPS induces EAMG. LPS-AChR induced EAMG shares several characteristics in common with MG, such as the presence of high-affinity anti-AChR Ab in serum, deposition of IgG and complement at NMJ, decrease in the functional AChR at post-synaptic membrane, destruction of the post-synaptic membrane folds (Chapter 2). However, the precise mechanism of LPS-AChR induced EAMG development is not known.

Activated CD4+ T helper cells regulate CSR in B cells in two ways (17). CD4+ T helper cells induce the expression of activation-induced cytidine deaminase (*AID*) in B cells by ligation of CD40 on B cells with CD154 (CD40L) expressed on activated T cells (54). AID is the enzyme responsible for *IgH* CSR in B cells. CD4+ T helper cells also influence CSR by secretion of cytokines, like IFN-γ and IL-12 which promote production of *IgH* of a particular class.

Recent research suggests the existence of another class switch recombination (CSR) pathway mediated by BAFF and APRIL, TNF family members (53, 54). BAFF and APRIL have been shown *in vitro* to stimulate purified human B cells and CD40 -/- mouse B cells to CSR (93). Expression of BAFF, an essential B cell survival factor, has been reported to be increased in the thymus of MG patients (15). TLR activation of the innate immune system induces inflammatory cytokines which stimulate macrophages and dendritic cells (DCs) to produce BAFF (51, 53, 94).

In this chapter, we investigated whether LPS-AChR immunization requires CD4+ T cells for the induction of EAMG. In this study, we show for the first time that LPS, when used as an adjuvant, can induce EAMG in CD4-/- mice. The comparison of humoral immune responses in both CD4-/- and WT mice post immunization with either CFA-AChR or LPS-AChR revealed that the mechanisms leading to autoimmunity in these two models are not identical.

RESULTS

Induction of EAMG in WT and CD4-/- mice

To determine whether LPS can enhance immune responses to AChR and induce similar clinical features of CFA-AChR-induced EAMG, C57BL6 mice were immunized s.c. with LPS (5μg) and AChR (20μg) emulsified in IFA. The clinical findings were compared to those in mice immunized with AChR emulsified in CFA (Figure 13). The incidence and severity of disease were similar in both LPS-AChR- and CFA-AChR-immunized mice. At day 28, mild symptoms were observed in approximately 50% of the

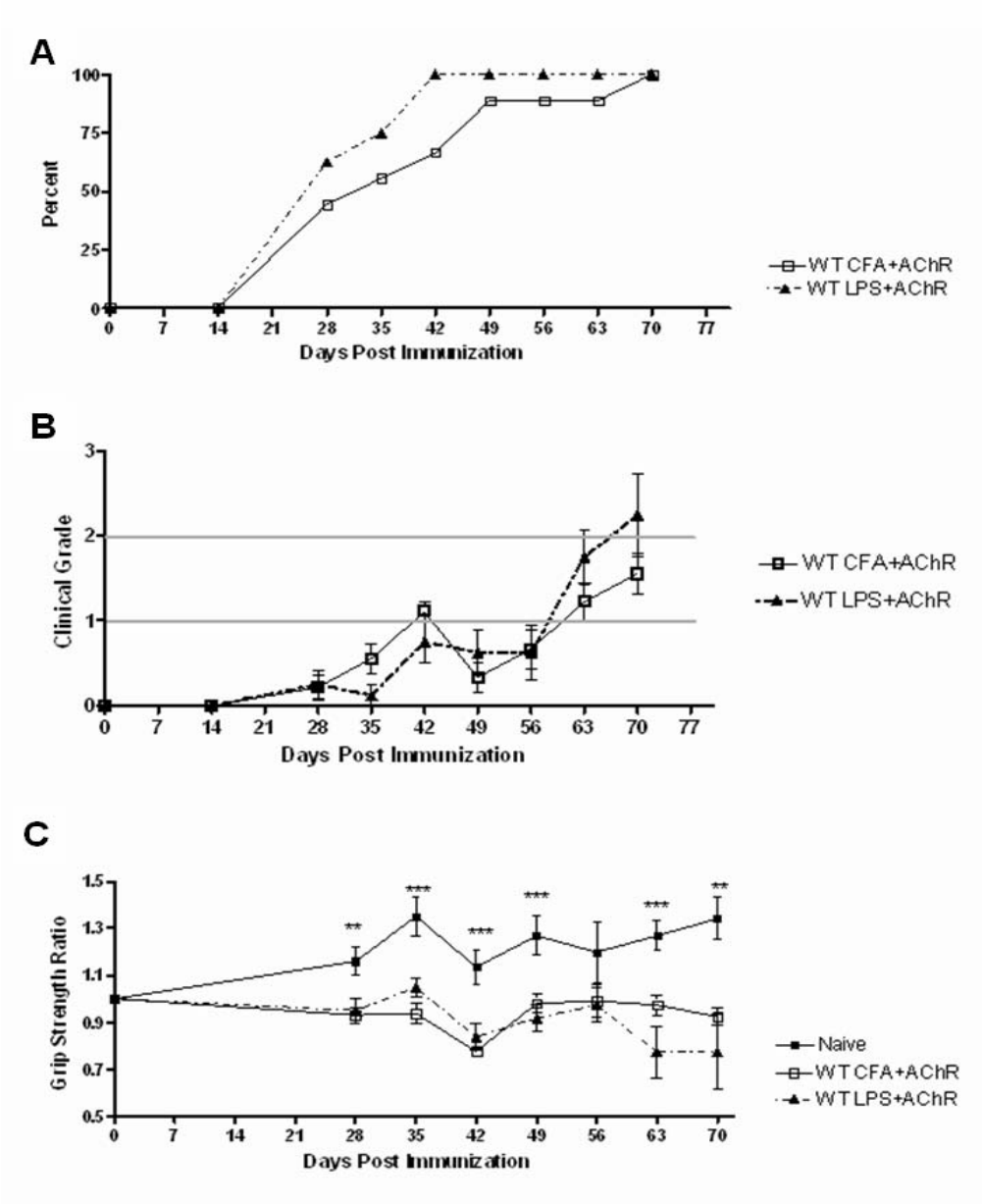

FIGURE 13: LPS-AChR-immunized mice develop clinical signs of EAMG. EAMG was induced in C57BL/6 mice by multiple immunizations with AChR in either CFA or in IFA with LPS. (A) Incidence is shown as percentage of mice with signs of EAMG. (B) The clinical grade of EAMG is shown as the mean clinical score (±s.e.m., n=10). (C) Grip-strength ratio is shown as mean ratio (±s.e.m., n=9). A Student's t-test was used at each time point to compare grip strength ratios of CFA-AChR and LPS-AChR-immunized mice to naïve mice,**p<.01, ***p<.001. Results shown represent one of three experiments performed simultaneously with CD4-/- mice.

mice. After the third immunization on day 56, 90% of the mice had moderate features of EAMG, characterized by hunchback posture, restricted mobility and decreased muscle grip strength after paw grip exercises. By day 70, several mice were dehydrated and moribund (clinical grade >2), and the study was terminated (Figure 13B). The kinetics of clinical severity in LPS-AChR- and CFA-AChR-immunized mice were remarkably similar, and at no time point was the clinical severity between the groups statistically different. An objective measure of muscle weakness in EAMG is to determine limb muscle strength overtime, as represented by the grip strength ratio (Figure 13C). A ratio > 1 indicates an increase in limb strength, and a ratio < 1 indicates a loss of limb strength. There was no significant difference in limb strength loss between the two models of EAMG (Figure 13C). Mice immunized with either CFA-AChR or LPS-AChR had a significant loss of limb muscle strength, compared to that in naïve mice at day 28 ($p=0.0052$), day 42 ($p<0.0001$), day 49 ($p<0.0001$), day 63 ($p=.0006$) and day 70 ($p=.0021$) (Figure 13C). These results are consistent with the data discussed in Chapter 2.

The CFA- AChR induced EAMG (CFA-EAMG) has been shown to be dependent upon the activation of AChR-specific CD4+ T cells. To determine the role of CD4+ T cells in LPS-induced EAMG, CD4-/- C57BL6 mice were immunized with AChR in CFA or LPS in IFA. The incidence and severity of disease varied significantly between the models of EAMG (Figure 14). At day 56 prior to a third boost, mild symptoms were observed in approximately 50% of CD4-deficient mice immunized with LPS-AChR, while CFA-AChR-immunized mice remained resistant to the induction of EAMG. CD4-deficient mice immunized with CFA-AChR also had no loss in limb strength throughout

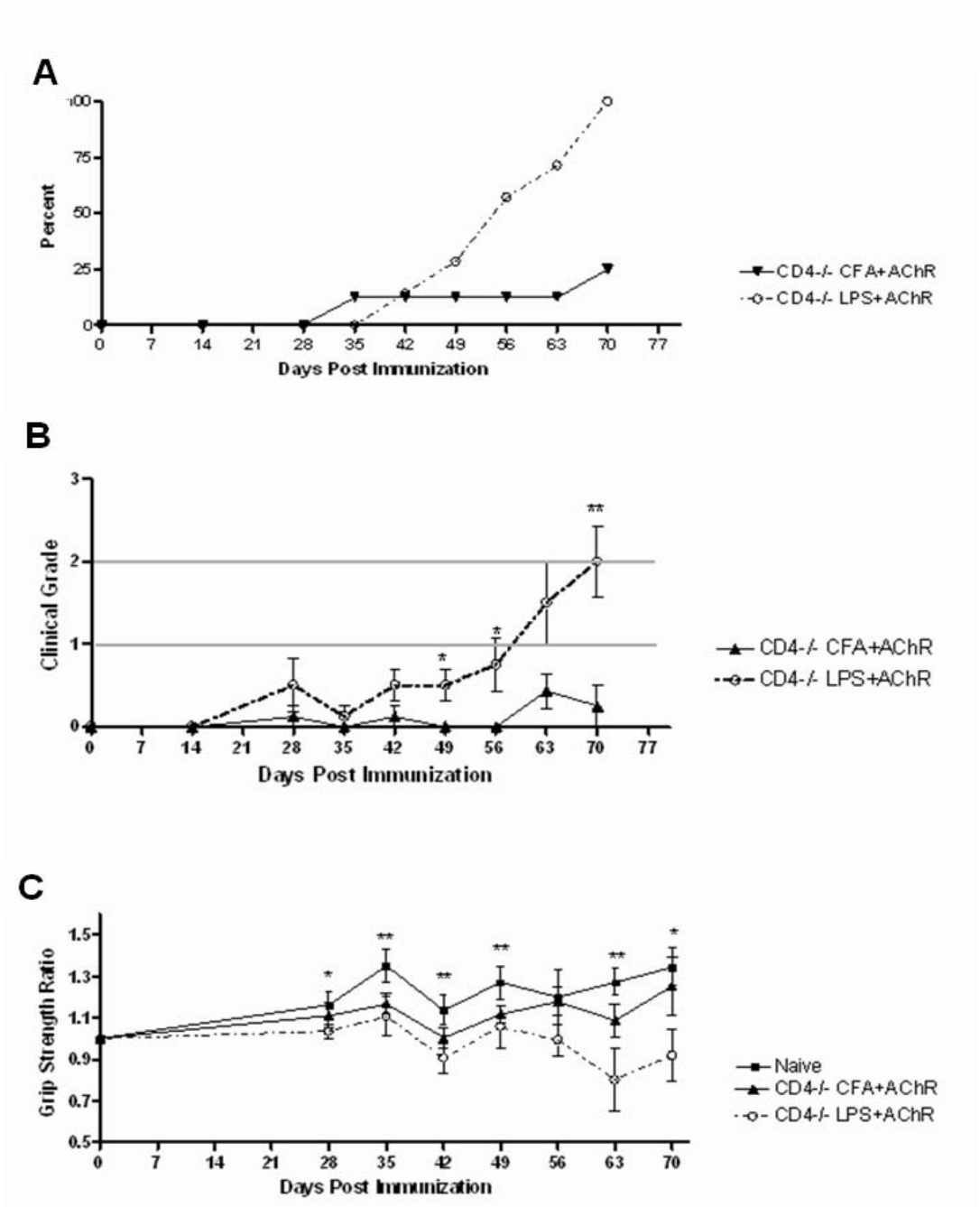

FIGURE 14: LPS-AChR immunization of CD4-/- mice induces EAMG. EAMG was induced in WT and CD4-/- C57BL/6 mice by multiple immunizations with AChR in either CFA or IFA with LPS. (A) Incidence is shown as percentage of mice with signs of EAMG. (B) Clinical grade of EAMG is shown as mean clinical score (±s.e.m., n=10, t-test, *p<.05. **p<.01). (C) Grip-strength ratio is shown as mean ratio (±s.e.m., n=10). *p<.05. **p<.01 (Student's *t*-test) indicates significant differences between grip strength ratios of LPS-AChR-immunized mice compared to naïve mice.

the course of the study (Figure 14C). By day 70, LPS-AChR-immunized, CD4-deficient mice had moderate features of EAMG comparable to clinical signs of EAMG in WT mice on day 70 (Figure 14B). Clinical grade of EAMG in LPS-AChR was more severe than in CFA-AChR-immunized mice on day 49 ($p=0.0453$), day 56 ($p=.032$), and day 70 ($p=0.0031$) (Figure 14B). In addition, mice immunized with LPS-AChR have significant loss of limb muscle strength, as was indicated by grip strength ratio <1 compared to that of naïve mice on day 28 ($p=0.05$), day 35 ($p=0.0062$), day 42 ($p=0.0067$), day 49 ($p=0.0029$), day 63 ($p=.0021$) and day 70 ($p=.0127$) (Figure 2C). These results show that significant clinical signs of EAMG were only observed in CD4-/- mice after immunization with LPS-AChR.

LPS-AChR-immunized CD4-/- mice produce significant amounts of class-switched anti-AChR antibodies

Anti-AChR antibodies are the main effector molecules responsible for the pathogenesis of MG and EAMG. The concentrations of anti-mouse AChR Abs were determined and compared between the models of EAMG (Figure 15). The LPS-AChR-immunized mouse sera had higher levels of anti-AChR IgM ($p<0.01$) and IgG2b ($p<0.01$), compared to the levels in naive mice regardless of the presence of CD4+ T cells. However, LPS-AChR-immunized mice do not produce significant amounts of anti-AChR IgG1. The CFA-AChR-immunized WT mice had significantly higher serum levels of anti-AChR IgG1 ($p<.001$) and IgG2b ($p<0.01$). The CD4-/- mice immunized with CFA-AChR did not produce significant amounts of anti-AChR IgM, IgG1, or IgG2b.

These data demonstrate that the immunization of mice with LPS-AChR induces the production of antibodies capable of recognizing AChR, and these antibodies undergo class switching.

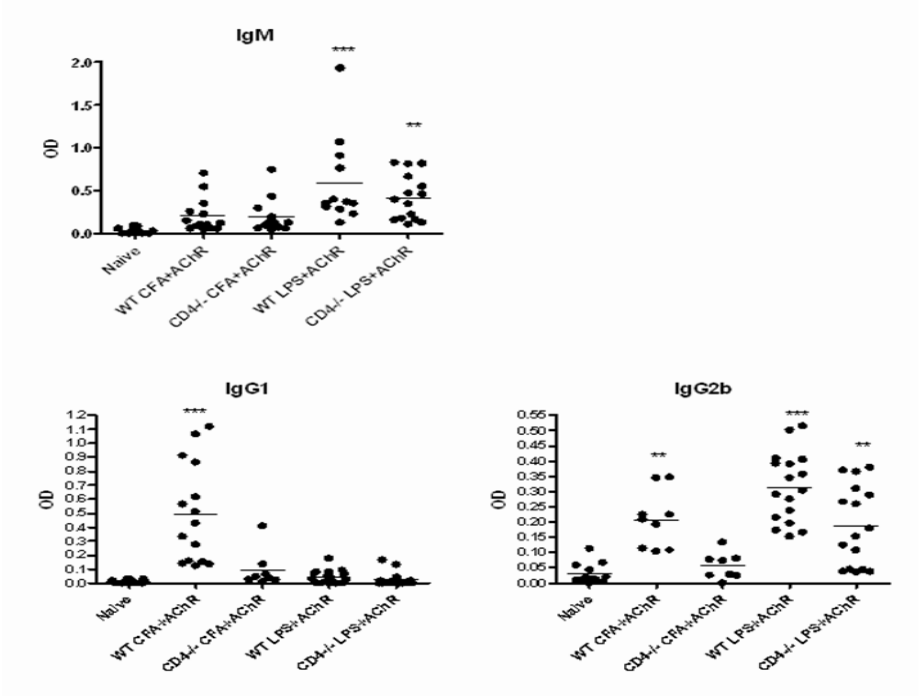

FIGURE 15: Serum anti-AChR IgG and IgM responses in WT and CD4-/- mice after LPS-AChR immunization. Anti-AChR responses in serum were measured 2 weeks post boost immunization by ELISA. OD values for each mouse are represented for IgM, IgG1, and IgG2b (n=10-15). Bar indicates mean OD. Statistical significance (*p<05, **p<.01, *** p<.001) was determined by Student's *t*-test comparing immunized to naïve mice. Results were combined from two-independent experiments.

LPS-AChR immunized CD4-/- mice produce significant amounts of high-avidity anti-AChR IgG2b antibodies

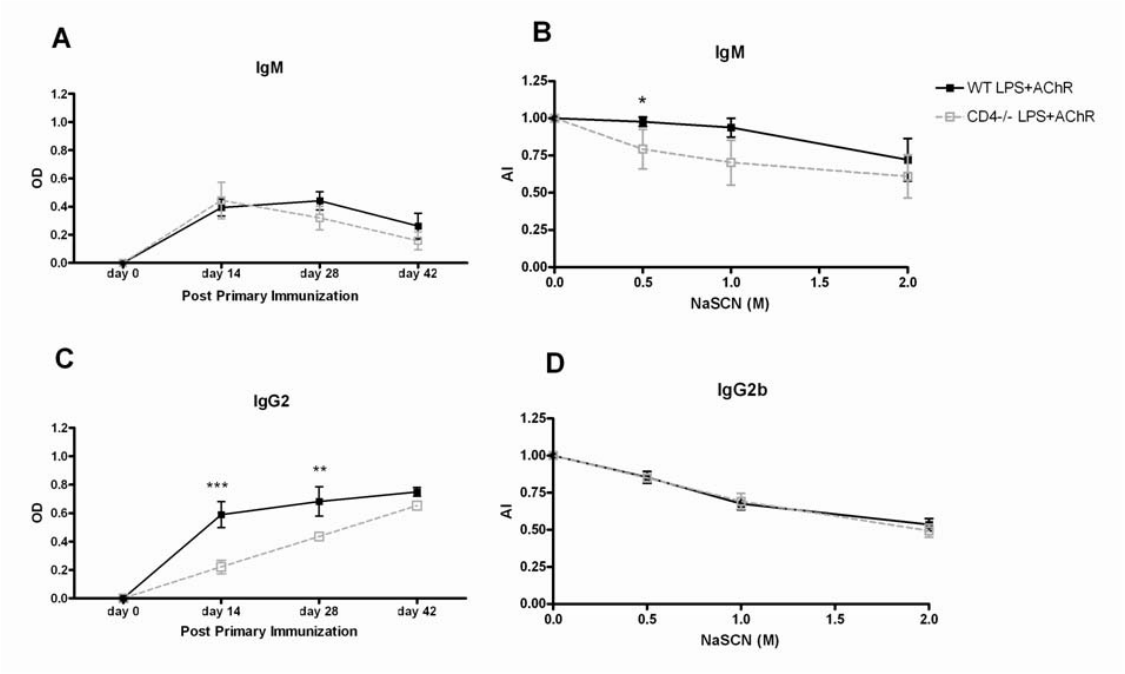

FIGURE 16: Kinetics and avidity of anti-AChR Abs in LPS-AChR immunized mice. (A) Anti-AChR IgM and (C) anti-AChR IgG2 levels were determined at various time points post primary immunization, shown as mean OD (s.e.m., n=10). (B) Mean AI of anti-AChR IgM and (D) anti-AChR IgG2b at day 42 post immunization (s.e.m., n=5-10). Statistical significance (*p<.05,**p<.01,***p<.001) was determined by Student's *t*-test. Results are representative of two independent experiments.

To characterize complement-fixing antibodies produced by LPS-AChR immunization, we next analyzed the kinetics of anti-AChR Ab production and the avidity of Abs. Sera anti-AChR IgM titers were significantly elevated by day 14 post-primary

immunization with no significant differences between WT and CD4-/- mice (Figure 16A). WT mice produced anti-AChR IgM Abs with a higher avidity for muscle AChR than did CD4-/- mice (Figure 16B). Avidity was not determined for CFA-AChR-immunized mice, since CD4-/- mice do not produce significant levels of anti-AChR IgM or IgG (Figure 16). The WT mice produced significantly higher titers of anti-AChR IgG2b by day 14 post immunization, when compared to the levels in CD4-/- mice immunized with LPS-AChR. The differences of anti-AChR IgG2b production between WT and CD4-/- mice decreased overtime (Figure 16C). The WT and CD4-/- mice had similar anti-AChR IgG2b avidity to muscle AChR (Figure 16D). Therefore, despite the initial lag in anti-AChR IgG2b production, CD4-/- mice were able to produce significant amounts of high affinity/avidity anti-AChR IgG2b after immunization with LPS-AChR.

The LPS-AChR- immunized CD4-/- mice had intense NMJ IgG2 and C3 deposits

AChR loss in MG and EAMG is mediated by complement-fixing IgG deposits at the motor end plate. Two complement-binding classes, IgM and IgG2, were significantly higher in the sera of LPS-EAMG compared to naïve mice (Figure 15). To determine which of these two antibody classes contribute to interference with AChR-signaling at the NMJ, frozen limb muscle sections were obtained from WT and CD4-/- LPS-AChR-immunized mice on day 70. Cryostat muscle sections were double stained with α-bungarotoxin (to locate AChR at the NMJ) and anti-IgG2, anti-IgM, or anti-C3 (to localize immune complexes in muscles) (Figure 17). IgG2 deposits were detected at NMJ of WT mice immunized with LPS-AChR or CFA-AChR. Similar staining of IgG2 was

observed in CD4-/- mice immunized with LPS-AChR. Fewer NMJ from CD4-/- mice immunized with CFA-AChR stained positive for IgG2, albeit at a significantly reduced intensity compared to that of LPS-AChR-immunized mice. This result was unexpected because anti-AChR antibodies were not detected by an ELISA in the sera of CFA-AChR-immunized CD4-/- mice (Figure 15). However, other groups have reported Abs from sera-negative patients with MG are able to bind AChR expressed by muscle tissue, but not AChR bound to ELISA plates. This is most likely due to the native conformation of AChR at the NMJ in tissue that cannot be replicated by ELISA techniques. IgM was not localized in the NMJs of LPS-AChR or CFA-AChR-immunized mice (Figure 17A and Figure 17B). In addition, C3 deposition merged with IgG2 deposits at the NMJ. LPS-AChR-immunized CD4-/- mice had NMJ with strong IgG2 staining and also had many C3-positive NMJ. CD4-/- CFA-AChR- immunized mice had fewer and less intense IgG2 deposits, which corresponded to an insignificant amount of C3 deposits (Figure 17B). This finding suggested to us that IgG2, and not IgM, could cross link AChR at NMJ and activate complement at the motor endplate, leading to defective neuromuscular transmission.

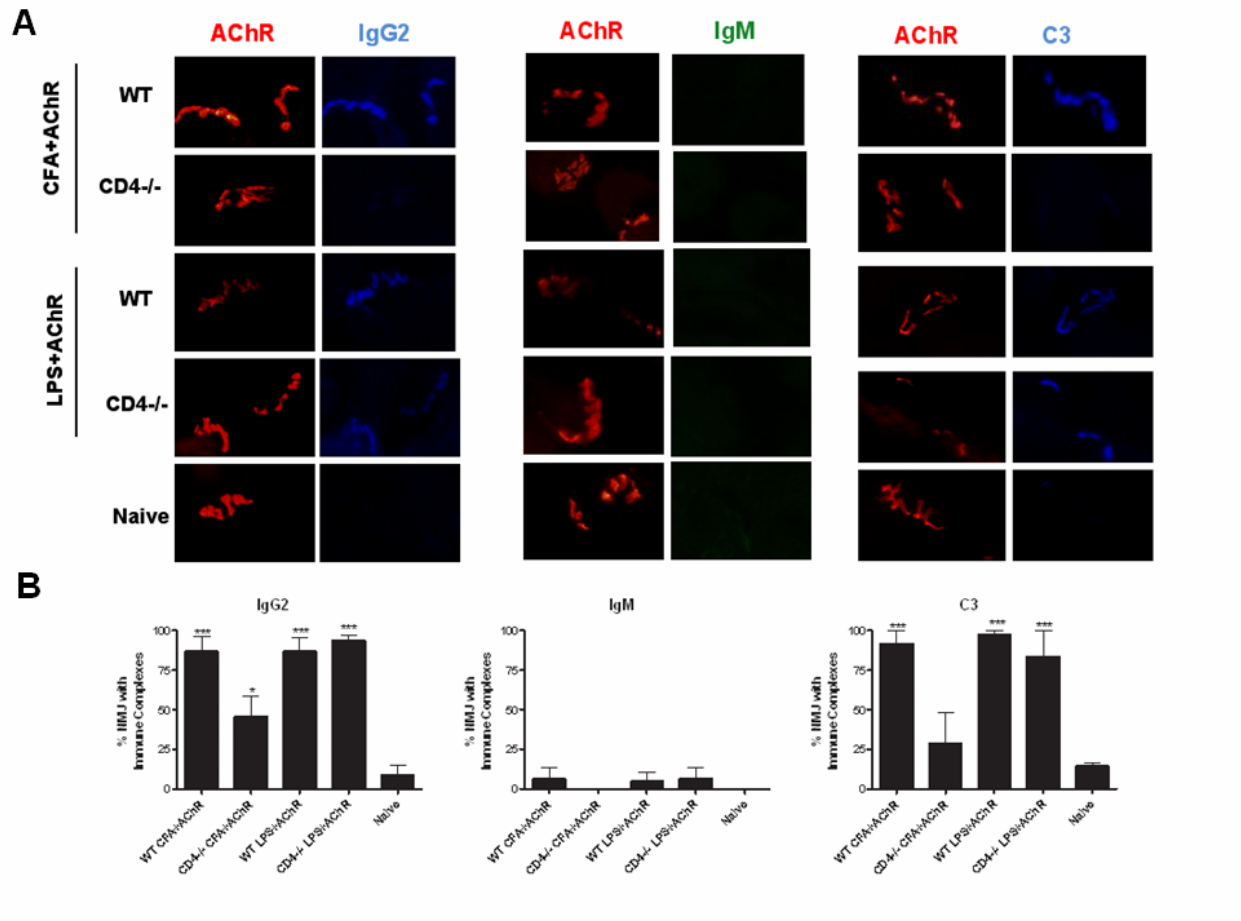

FIGURE 17: IgG2 and C3 deposition in the NMJ. EAMG was induced in WT and CD4-/- C57BL/6 mice by multiple immunizations with CFA-AChR or IFA-LPS and euthanized on day 80 post-primary immunization. Control mice were unimmunized. (A) Cryostat sections of right tricep mucle were co-stained with α-bungarotoxin to identify AChR (red) and either anti-mouse IgG2 (blue), anti-mouse IgM (green), or anti-mouse C3 (blue).Data shown are representative of sections obtained from several mice from each group (n =5). Original 200 X magnification. (B) Mean percentage of NMJ with immune complexes (n=5, Student's *t*-test, * $p<0.05$, ***$P<0.001$).

The CD4-/- mice have elevated frequencies of AChR-specific IgG expressing B cells

B cell activation resulting from LPS-AChR immunization of WT and CD4-/- mice lead to the secretion of anti-AChR IgG2 in blood and copious amounts of immune complex deposition in muscle. The B cell activation resulting from CFA-AChR immunization of CD4-/- mice was significantly impaired, as evident by the significant reduction in anti-AChR IgG2 secretion and reduction of immune complexes detected in muscle. However, it is not clear whether the differences observed were due to a poor primary immune response of naïve AChR-specific B cells resulting in fewer activated AChR-specific B cells or whether the lack of CD4 lead to deletion of activated B cells, altered cellular differentiation, or B cell anergy. To determine the extent of B cell activation by CSR to IgG in CD4-/- mice, we utilized a flow cytometry assay to detect circulating AChR-specific B cells (Chapter 4). Alexa fluor-AChR was used as a probe for potentially autoreactive AChR-specific B cells in peripheral blood of immunized mice. Lymphocytes were gated on B220+ cells, and then expression of Ig and binding of AChR were compared (Figure 18). There were no significant differences in the total frequencies of B cells (B220+ lymphocytes) present in blood of naïve, WT CFA-AChR, WT LPS-AChR, CD4-/- CFA+AChR, and CD4-/- LPS-AChR immunized mice (data not shown). All mice immunized with AChR regardless of genotype or adjuvant used had significantly elevated frequencies of AChR-binding B cells compared to naïve mice.

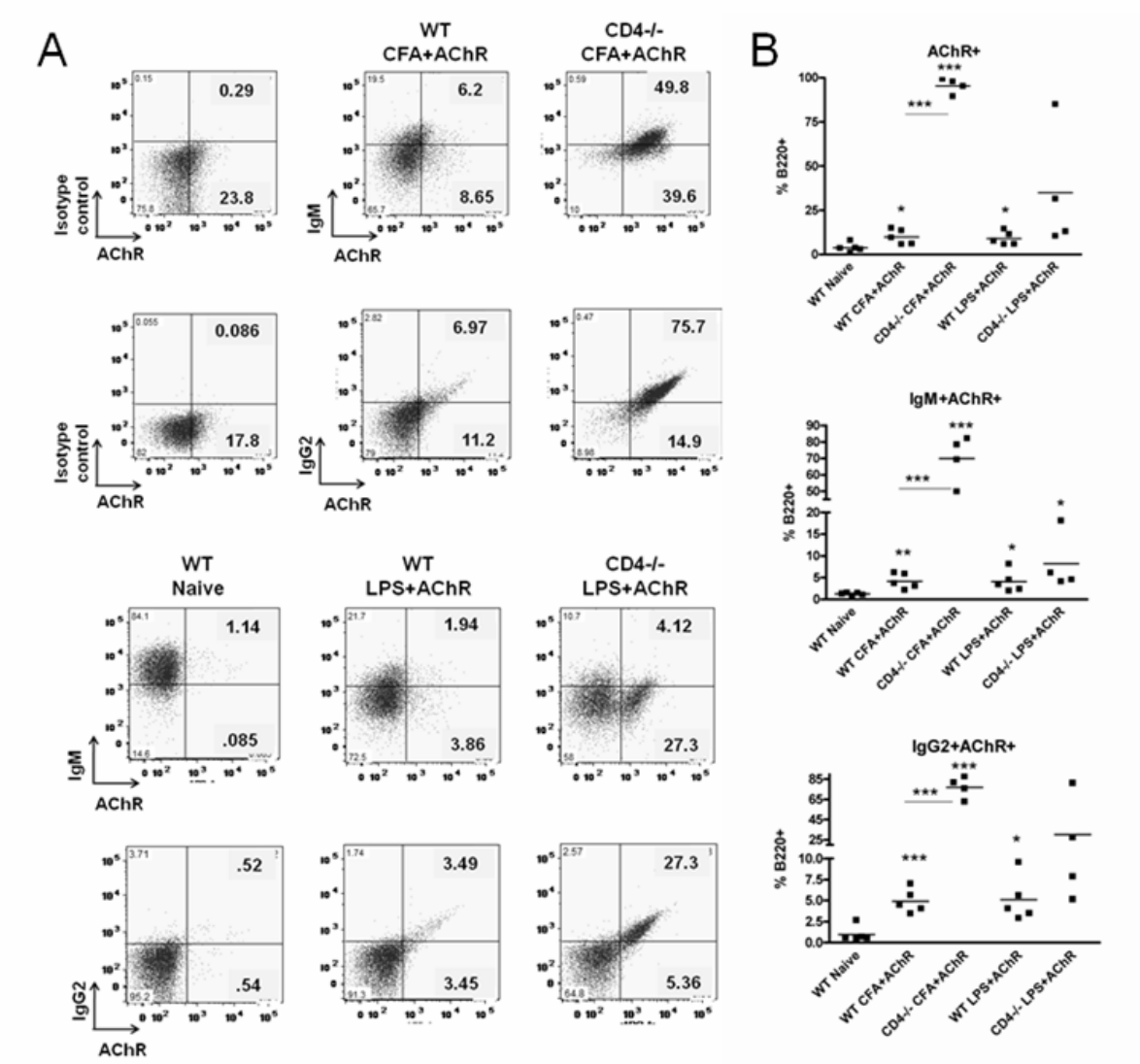

FIGURE 18: The frequencies of AChR-binding peripheral blood lymphocytes are elevated in CD4-/- mice. Representative flow cytometry analysis of peripheral blood lymphocytes from naïve, LPS-AChR or CFA-AChR-immunized mice, 75 days post primary immunization. Cells were first gated on B220+ lymphocytes to characterize IgM or IgG2 expression and AChR binding (A). The numbers shown in bi-exponential plots indicate the relative percentage of cells in each quadrant. Mean frequency of total AChR-binding B cells (top row), IgM+ AChR-binding B cells (middle row) and IgG2+ AChR-binding B cells (bottom row) (B). n=4-5, Student's *t*-test, * $p<0.05$, ***$P<0.001$.

Of particular interest, both LPS-AChR and CFA-AChR immunized CD4-/- mice had higher mean frequencies of AChR-binding B cells than naïve, WT CFA-AChR, and WT LPS-AChR immunized mice. However, the frequency of AChR+ peripheral B cells was in the highest in CD4-/- CFA-AChR immunized mice (Figure 18). Therefore, it is likely that cells from CFA-AChR immunized CD4-/- mice are not deleted but, may be either inhibited from differentiating into antibody secreting plasma cells or perhaps preferentially shunted into the memory B cell repertoire and are anergic. The differences in B cell subsets may be more dependent upon signals provided by adjuvant than CD4 costimulation, since LPS-AChR immunized CD4-/- mice are capable of producing high affinity secreted IgG.

Potential role of adjuvant-induced expression of CD40L and BAFF in determining B cell differentaition

The maturation of antigen-specific B cell responses requires activation of CD40 via CD40L expressed by T cells. CD40L is preferentially expressed by activated TCRαβ T cells which consist of CD8+ T cells, CD4+ T helper cells, and CD4+ T regulatory cells. To determine if there was an adjuvant specific difference in the expression of CD40L, we measured the frequencies of lymphocyte subsets in draining lymph nodes of LPS or CFA plus AChR immunized mice by flow cytometry (day 80). There was no significant difference in the frequency of TCRαβ+ cell subsets between LPS-AChR and CFA-AChR

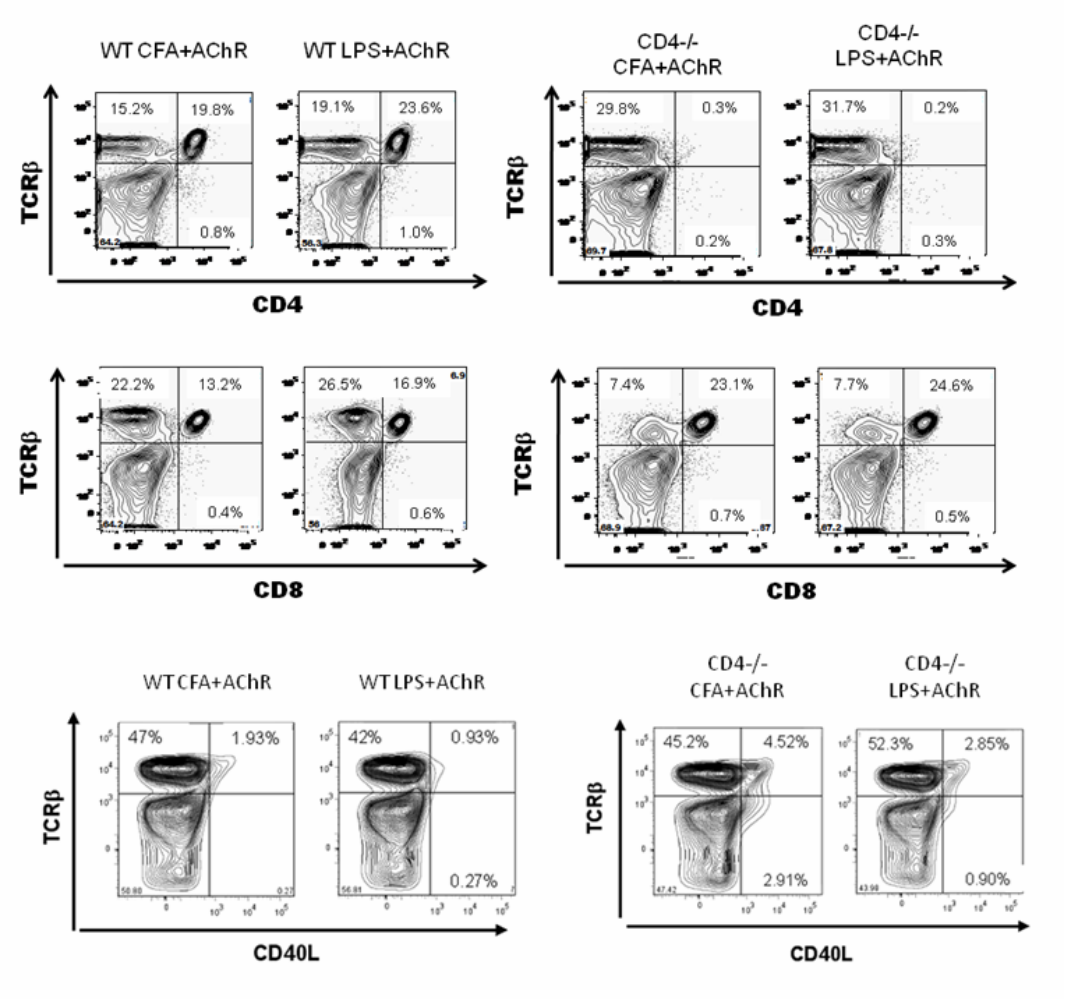

FIGURE 19: Flow cytometry analysis of T lymphocyte subsets and expression of CD40L. Representative flow cytometry analysis of LN cells from naïve, LPS-AChR or CFA-AChR-immunized mice, 80 days post primary immunization. Lymph node cells from indicated immunization procedure and genotype at the top of figure were stained with anti-TCRβ, anti-CD4, and anti-CD8 or anti-TCRβ and anti-CD40L. The numbers shown in bi-exponential plots indicate the relative percentage of cells in each quadrant.

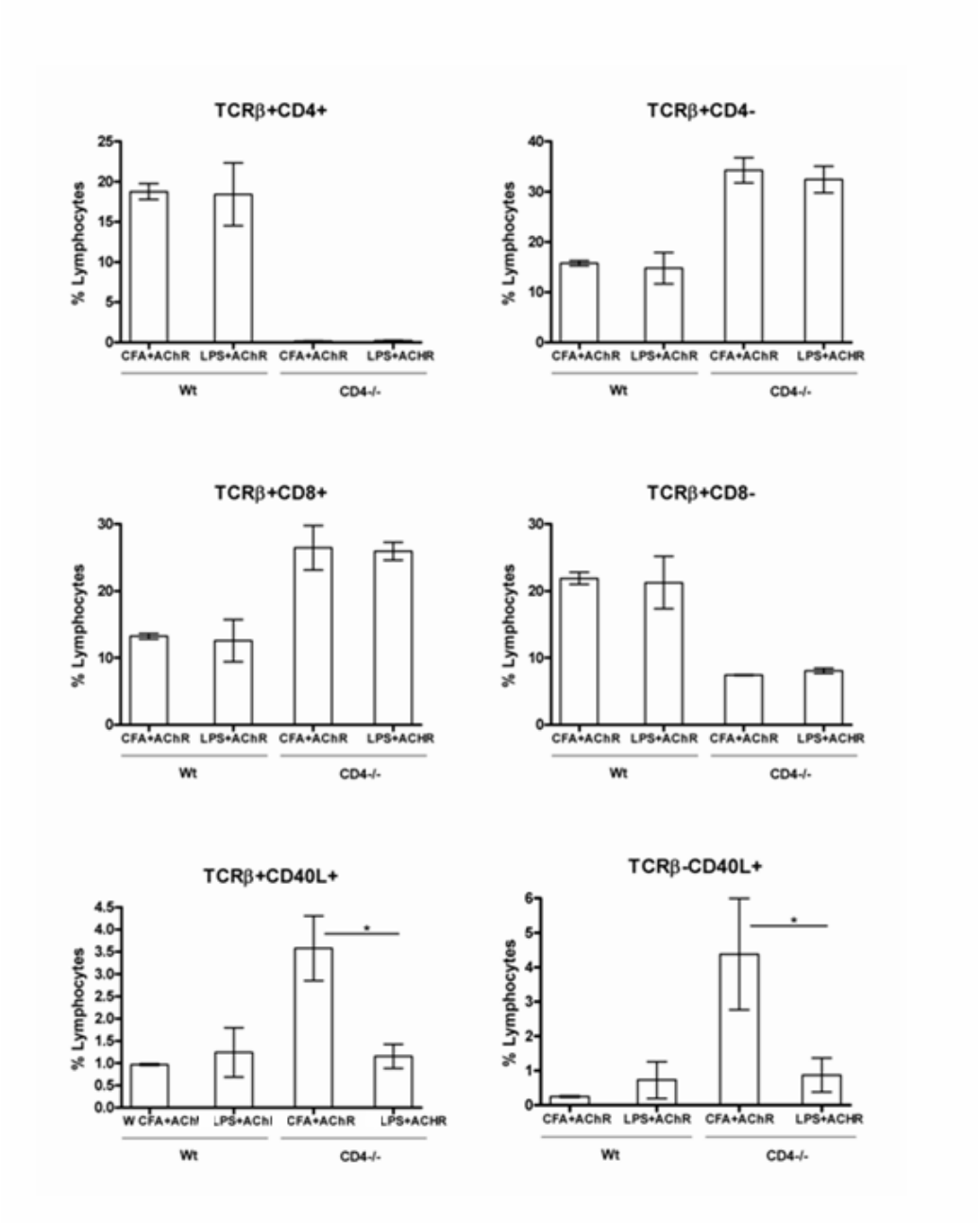

FIGURE 20: Lymph node T cell subsets and expression of CD40L on day 80 post immunization. Lymph node cells were stained with anti-TCRβ, anti-CD4, and anti-CD8 or anti-TCRβ and anti-CD40L. Shown is the mean percentage of each subset with SEM (n=3). Data are representative of two independent experiments.

immunized WT mice. As expected, CD4-/- mice had significantly higher frequencies of TCRβ+CD8+ and lower TCRβ+CD4+ than did WT mice (Figure 19). Of particular interest, the EAMG-resistant CD4-/- mice immunized with CFA-AChR but not LPS-AChR had significantly higher frequencies of TCRαβ+CD40L+ cells and TCRαβ-CD40L+ (Fig. 19 and Figure 20). Therefore, immunization of CFA-AChR, but not of LPS-AChR, augmented the expression of CD40L in CD4-/- mice, which coud have contributed to the altered B cell differentiation in these mice.

B cells also require cytokines to promote CSR and cellular differentiation. Among the cytokines we measured by ELISA (IL-6, IL-10, IFN-γ and BAFF) two weeks following each immunization, only BAFF was detectable in the sera of mice (data not shown). BAFF is a B cell survival factor that is critical for the maintenance of peripheral B cells. Elevated BAFF sera levels have been observed in MG patients, as well as in other autoimmune diseases. The *in vitro* studies in mouse and human B cells have shown that stimulation of B cells with BAFF induces T cell-independent isotype switching and B cell survival. Sera BAFF levels in mice immunized with LPS-AChR were significantly higher than naïve and CFA-AChR immunized mice (Fig. 21A). AChR-immunized CD4-/- and WT mice produced similar amounts of BAFF. Therefore, the CD4 expression on cells does not alter BAFF production. These findings suggest that LPS-AChR induces BAFF expression in C57Bl6 mice more effectively than does CFA-AChR immunization. Next we compared individual sera anti-AChR IgG2 titers to BAFF sera concentrations to determine whether the differences in sera BAFF production correspond to B cell differentiation into anti-AChR IgG2 secreting cells. LPS-AChR sera BAFF

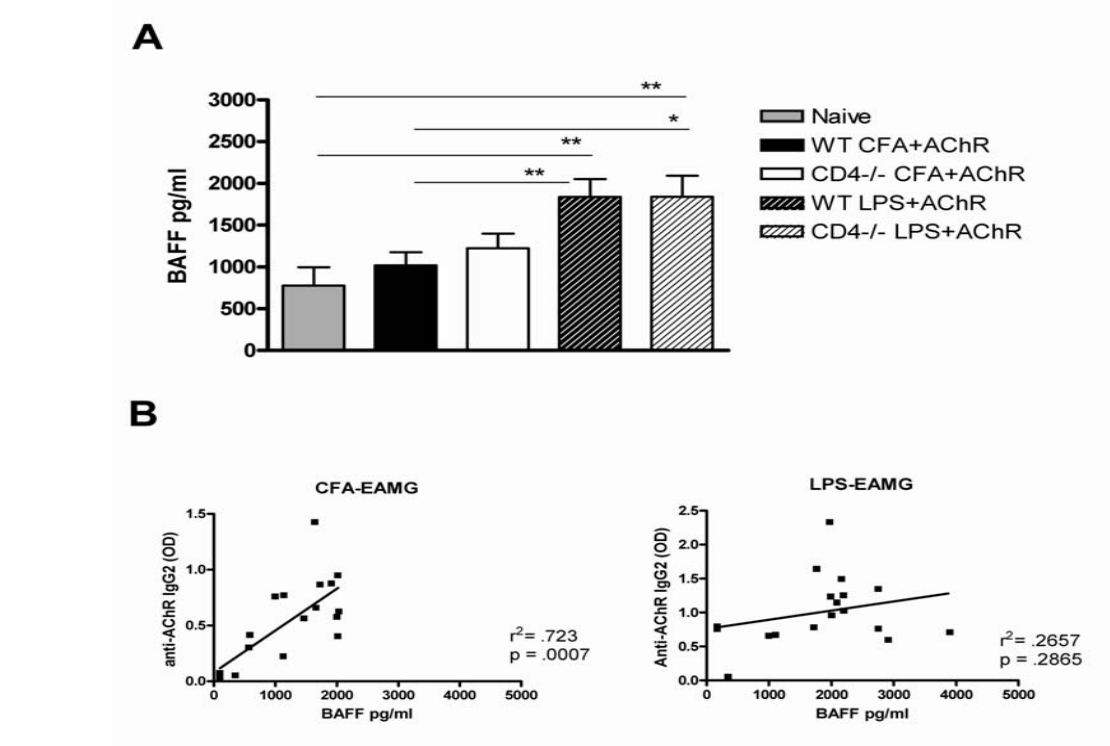

FIGURE 21: Adjuvant-specific induction of BAFF and correlation with anti-AChR IgG2 secretion. EAMG was induced in C57BL/6 mice by multiple immunizations with LPS-AChR or CFA-AChR. Serum concentrations of BAFF and anti-AChR IgG2 were measured 14 days post boost immunization by ELISA. Mean concentration of BAFF is shown with SEM (n=6-10) (A). Results were combined from two-independent experiments. Statistical significance was determined for each group with EAMG vs naïve mice by Students's *t*-test,* p<.05,**p<.01. Sera anti-AChR IgG2 titers (OD) versus BAFF concentration (B). Each square represents data from individual mice (n=18). R, represents the Pearson coefficient.

concentrations, which are significantly elevated compared to naive and CFA-AChR immunized mice, do not correlate well with anti-AChR IgG2 titers (r =2657, p = .2865, n=18). However, CFA-AChR immunized mice have lower concentration of sera BAFF which significantly correlates with anti-AChR IgG2 titers (r = .723, p=.0007, n=18) (Fig. 21B).

DISCUSSION

Previously, the adjuvant effect of LPS was demonstrated in various models of autoimmunity, including those for experimental autoimmune thyroiditis, experimental autoimmune arthritis, and lupus-prone MRL/lpr mice (57, 61, 62). In both Chapter 2 and 5, we demonstrated the use of LPS in place of desiccated *Mycobacterium* as an adjuvant for immunization with AChR in incomplete Freund's adjuvant. In the current study, both, WT and CD4-/- mice were susceptible to LPS-AChR- induced EAMG. However, the time of EAMG onset was delayed about 14- 21 days in CD4-/- mice immunized with LPS-AChR. The WT and CD4-/-mice immunized with LPS-AChR produced significant amounts of IgM and IgG2. The CD4 deficiency had no effect on the production of anti-AChR IgM throughout the course of disease in LPS-AChR- immunized mice. Therefore, the delay in disease onset corresponded to the altered kinetics on anti-AChR IgG2 production in CD4-/- mice. However, by day 42 sera anti-AChR IgG2 levels were similar to that of WT mice. Muscle weakness was also associated with the deposition of IgG2 and C3 at the NMJ. Maturation of antibody responses was measured by avidity of anti-AChR IgG and was found to be equally robust in WT and CD4-/- mice.

The significance of the elevation of anti-AChR IgM in LPS-induced EAMG is not known, since it is not directly involved in the binding of AChR at the NMJ. However, IgM may play a key role in augmenting immune responses towards AChR. The IgM opsinization of AChR and activation of complement may increase AChR uptake by antigen- presenting cells (APCs) conferring enhanced activation of APCs (21). Also complement receptor (CR2/CR1) stimulation of B cells was reported to lower BCR

activation thresholds by 1000-fold (95). Recent studies have also suggested that complement-opsonized molecular mimics to self antigen can reverse B cell anergy (96).

CD4 deficiency alone leads to resistance to EAMG induction following CFA-AChR immunization. These data are in agreement with previous studies of CFA-AChR induced EAMG (89, 90, 97). However, our data indicates that the dependency of CD4 costimulation of B cells may be dependent upon the stimuli present (*Mycobacterium* or LPS) during B cell activation. Futhermore, our studies show that both LPS-AChR and CFA-AChR immunized CD4-/- mice had higher mean frequencies of IgG expressing AChR-binding B cells than WT mice treated in the same manner. This difference was exacerbated in CFA-AChR immunized CD4-/- mice. However, B cells from CD4-/- mice immunized with CFA-AChR failed to differentiate into antibody secreting cells. These data suggest that the lack of anti-AChR IgG secretion by CFA-AChR immunized CD4-/- mice was not due to an inability to activate naïve B cells, inefficient CSR or deletion of autoreactive B cells. Therefore, B cells from CFA-AChR immunized CD4-/- mice are either inhibited from differentiating into antibody secreting plasma cells or perhaps preferentially shunted into the memory B cell repertoire which may be anergic.

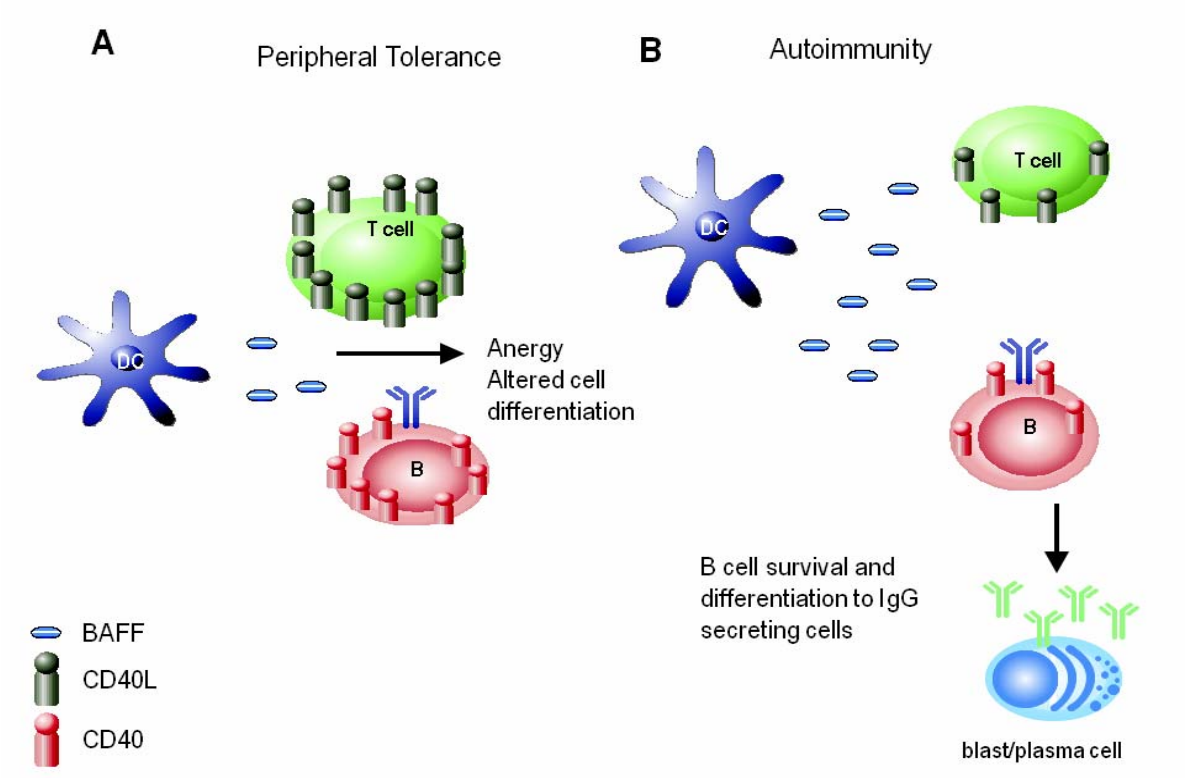

FIGURE 22: A hypothetical model for the regulation of peripheral B cell tolerance in EAMG. (A) In EAMG resistant mice activated T cells express high levels of the costimulatory activation marker, CD40L. When BAFF concentration is near normal range, the elevated CD40L-CD40 interactions trigger cell cycle arrest inducing a state of anergy or inhibiting B cell differentiation. (B) In EAMG prone mice, T and B cells express lower levels of CD40L and have normal to significantly elevated BAFF concentrations. The elevated proportion of BAFF compared to CD40-CD40L signals provides appropriate activation for B cell differentiation into antibody secreting cells.

It is still not understood how people with MG manage to bypass peripheral tolerance checkpoints and why AChR specifically is targeted. The thymus is considered by many to be the site of autosensitization to AChR where both thymic myoid cells and thymic epithial cells have been shown to express AChR (12). Approximately 80% of MG patients have thymic abnormalities, such as thymitis, thymoma, or involusion. In addition to MG patients, those with systemic lupus erythematosus rheumatoid arthritis, and rheumatic heart disease, among other autoimmune conditions, manifest similar thymic abnormalities (16). Since the thymus is a primary immune organ responsible for T cell development and selection, thymic abnormalities may alter the selection of the developing T cell repertoire (13). In particular, CD4+ T cells may have a crucial role in the induction of peripheral B cell tolerance. It has been demonstrated that excess CD40L expression by CD4+ T regulatory cells induces deletion of B cells by Fas-mediated apoptosis (98, 99). Furthermore, CD40L-deficient patients have significantly lower frequencies of CD4+ T regulatory cells and elevated peripheral autoreactive B cell populations (100). Taken together, a CD4 deficient model of autoimmunity may be valuable in understanding the underlying mechanisms leading to diseases such as MG.

The production of matured antibody responses, defined here by the presence of secreted high-affinity IgG, by LPS-AChR-immunized CD4-/- mice, indicated the involvement of CD40-CD40L interactions. LPS-AChR-immunized CD4-/- mice had similar levels of CD40L compared to those in WT- immunized mice. CD4-/- CFA-AChR-immunized mice, which were resistant to EAMG induction, had significantly elevated expression of CD40L compared to WT CFA-AChR immunized mice and LPS-

AChR immunized CD4-/- mice. These data indicate that excess CD40-CD40L signaling may inhibit or alter B cell differentiation in CFA-AChR-immunized CD4-/- mice.

BAFF also contributes to CSR and B cell survival (54). BAFF has been shown to be elevated in the thymus and sera of MG patients (15, 101). Excess BAFF levels have been shown to rescue autoreactive B cells from deletion and to prevent anergy (102). In this study, BAFF sera levels were found to be significantly elevated in mice immunized with LPS-AChR, compared to naïve and CFA-AChR-immunized mice. In addition, there is a significant correlation between sera anti-AChR IgG2 titers and BAFF in CFA-AChR immunized mice but no such correlation was observed in LPS-immunized mice.

In conclusion, these data indicate that autoimmune development triggered by LPS or CFA occur by activation of distinct B cell differentiation pathways. The CFA immunization requires CD4 costimulation of B cells to induce anti-AChR IgG2 secretion and does not significantly induce BAFF production. LPS immunization does not require CD4 costimulation to induce anti-AChR Ab secretion and significantly induces BAFF production. Taken together, the data suggest that the balance of CD40L signaling and survival signals from BAFF may facilitate the differentiation of autoreactive B cells into Ab secreting cells. We propose that this mechanism is critical for EAMG development in LPS-AChR- immunized mice (Figure 22). Further immunological investigation of these two models would increase our understanding of the pathways that lead to the activation, survival and differentiation of autoreactive B cells.

Chapter 6: The Effect of CD8 Deficiency on Anti-AChR Ig Responses in LPS-AChR Induced EAMG

INTRODUCTION

In the previous chapter we discussed the contribution of CD4+ T cells in the development of both CFA-AChR and LPS-AChR induced EAMG. However, CD8+ T cells may also contribute to the pathogenesis of organ-specific autoimmune diseases, such as MG, by various mechanisms. Autoreactive CD8+ T cells recognize Ag via MHC class I-peptide complexes on the surface of cells which triggers cell-mediated cytotoxicity either by expression of FASL or by the release of the cytotoxic granules, perforin and granzyme (103). Activated CD8+ T cells also secrete significant amounts of proinflammatory cytokines, TNF-α and IFN-γ (104). Suppressor CD8+ T cells may also regulate immune responses of CD4+ T cells by inhibiting costimulatory molecule expression on APCs or by the direct lysis of Ag-specific CD4+ T cells (105).

The exact role that CD8+ T cells in the induction of autoimmune responses remains elusive. This is due to contradictory results obtained from in EAE, non-obese diabetic (NOD) mice, and EAMG (103, 106). CFA-AChR immunization of MHC class I deficient mice was reported to enhance the progression of EAMG (107). Others reported that CD8-/- mice and CD8 Ab depletion of T cells decreased the severity of CFA-AChR induced EAMG (90). In CFA-induced EAT, CD8+ T cells are required for the induction of disease (108). However, CD8+ T cells were not required for the induction of LPS-induced EAT (63). There are no studies to date that evaluated the role of CD8+ T cells in

LPS-AChR induced EAMG. In this chapter we investigated anti-AChR Ig responses and the susceptibility of CD8-/- mice to develop LPS-AChR induced EAMG.

RESULTS

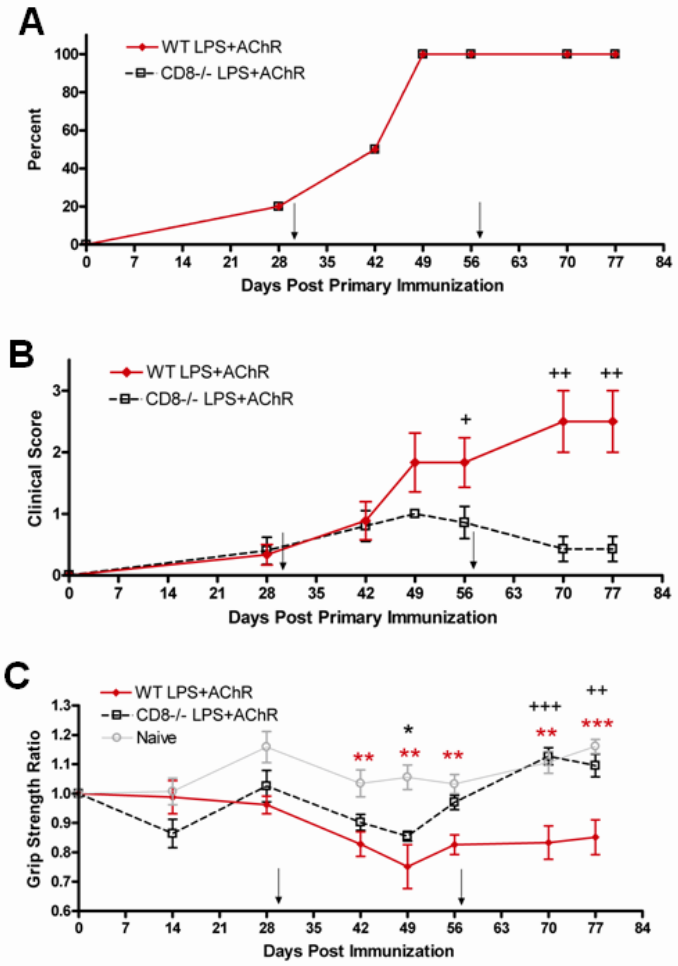

FIGURE 23: CD8-/- mice are resistant to LPS-AChR induced EAMG. (A) Incidence is shown as percentage of mice with signs of EAMG. (B) Clinical grade of EAMG is shown as mean clinical score (±s.e.m., n=10, t-test, +p<.05. ++p<.01). (C) Grip-strength ratio is shown as mean ratio (±s.e.m., n=10). *p<.05. **p<.01, **p<.001 (Student's *t*-test) indicates significant differences between grip strength ratios of LPS-AChR immunized WT mice compared to naïve. ++ p<.01, +++p<.001 indicates differences between LPS-AChR immunized WT and CD8-/- mice.

LPS-AChR immunization of CD8-/- mice induces EAMG with remission

The incidence and severity of muscle weakness after first boost with LPS-AChR was similar between WT and CD8-/- mice (Figure 23). By day 49, mild symptoms were observed in all immunized mice with a significant difference in muscle weakness, measured by grip strength ratio, compared to naïve mice (Figure 23C). However, at day 56, CD8-/- mice began to show signs of improved muscle strength which continued for the duration of the experiment. After day 56, CD8-/- mice had significantly reduced signs of EAMG and had a significant increase in grip strength compared to LPS-AChR immunized WT mice.

Since anti-AChR Abs are the main effector molecules responsible for the pathogenesis of MG and EAMG, we determined whether CD8 deficiency altered Ab production. The LPS-AChR-immunized mouse sera had higher levels of anti-AChR IgM, IgG1, IgG2 (b and c) at day 42 compared to the levels in naive mice regardless of the presence of CD8+ T cells (Figure 23). There were no significant differences in the quantity of anti-AChR Ab production between WT and CD8-/- LPS-AChR. We also determined sera anti-AChR Ab levels at day 75, a time point when disease severity was significantly different between WT and CD8-/- immunized mice, but no differences were observed (data not shown). These data indicate that the immunization of CD8-/- mice with LPS-AChR induces the production of Abs capable of recognizing AChR, however it may be possible that CD8 deficiency altered Ab avidity for AChR. By day 42, both WT

and CD8-/- immunized mice, produced anti-AChR IgM with strong avidity for AChR (Figure 25A). There was also no significant difference in the avidity of anti-AChR IgG2 between WT and CD8-/- immunized mice at day 42 (Figure 25B). We have shown in Chapter 4 and 5 that anti-AChR IgG2 Abs critical for the development and severity of

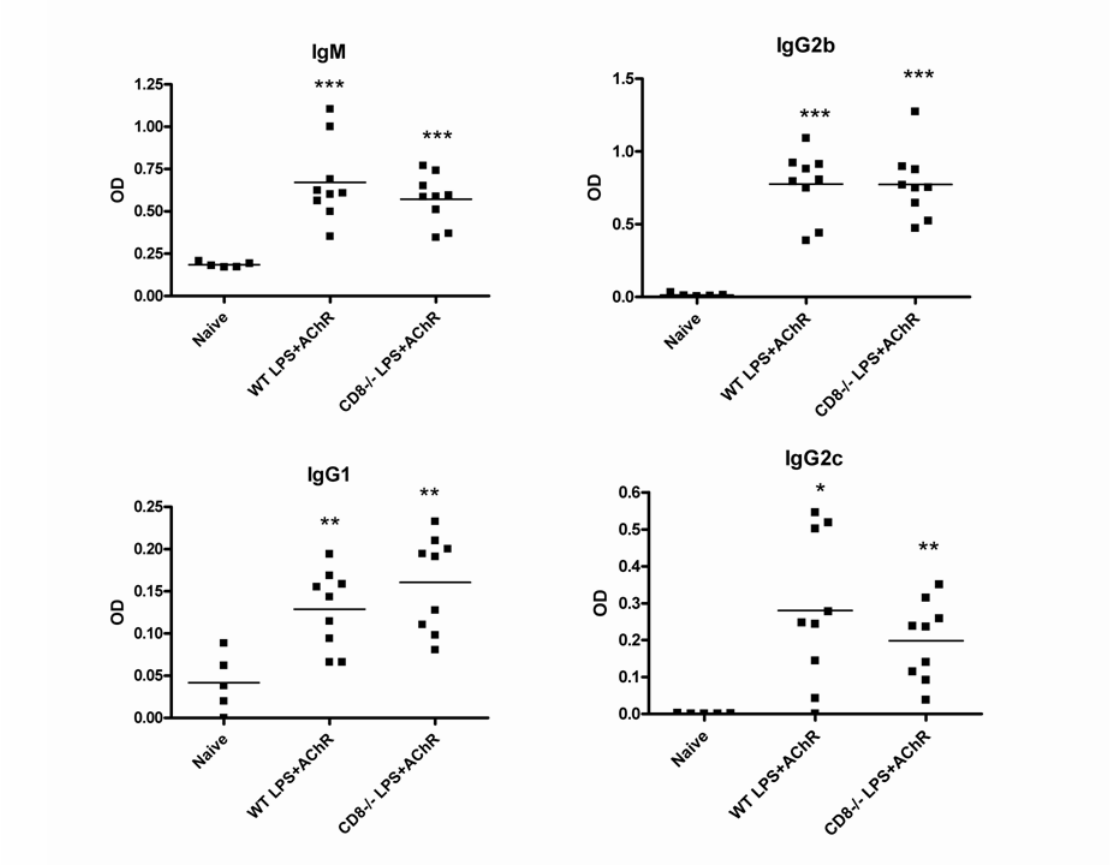

FIGURE 24: Serum anti-AChR IgG and IgM responses in WT and CD8-/- mice after LPS-AChR immunization. Anti-AChR responses in serum were measured 2 weeks post boost immunization by ELISA (day 42). OD values for each mouse are represented for IgM, IgG1, IgG2b and IgG2c ((n=5-10). Bar indicates mean OD. Statistical significance (*p<05, **p<.01, *** p<.001) was determined by Student's *t*-test comparing immunized to naïve mice.

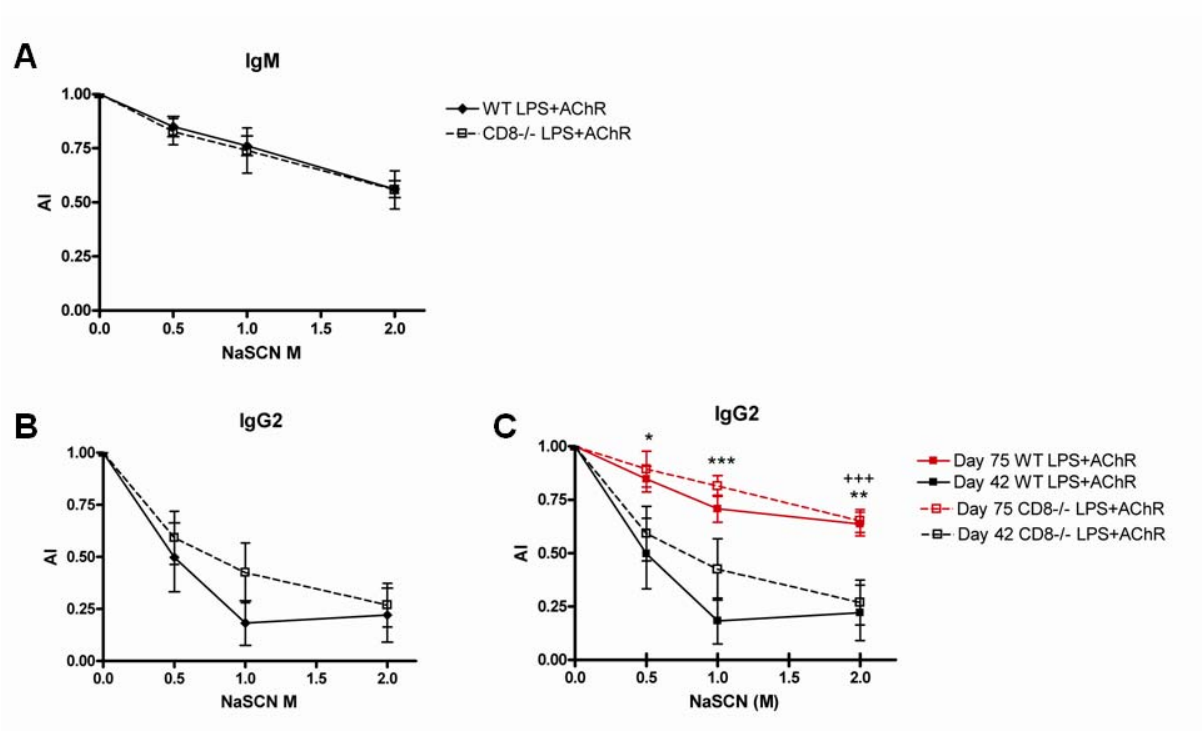

FIGURE 25: Avidity of anti-AChR IgM and IgG2 in LPS-AChR immunized CD8-/- and WT mice. (A) Mean AI anti-AChR IgM (B) anti-AChR IgG2 at day 42 post immunization (s.e.m., n=5-10) and (C) anti-AChR IgG2 at day 42 and 75 post immunization. Statistical significance (*p<.05,**p<.01,***p<.001) was determined by Student's *t*-test comparing WT and CD8-/- mice.

EAMG. Therefore, we compared the avidity of IgG2 Ab at day 42 to day 75, to determine whether CD8-/- mice had a defect in the selection of high-affinity Abs over time. However, both WT and CD8-/- mice produced IgG2 with significantly higher avidity for AChR at day 75 compared to day 42. These data suggests that the resistance to

EAMG in CD8-/- mice is not due to defects in anti-AChR IgG secretion or maturation of high-avidity Abs.

Cryostat muscle sections were double stained with α-bungarotoxin (Btx) and anti-IgG2, anti-C3, or anti-MAC (to localize immune complexes in muscles) (Figure 26). Immune complexes were detected at NMJ of WT and CD8-/- mice immunized with LPS-AChR. This result was unexpected because CD8-/- mice do not show signs of EAMG but have similar amounts of immune complexes deposited in muscle. However, since CD8-/- mice had similar levels of anti-AChR IgG2 and immune deposits in muscle compared to WT LPS-AChR immunized mice, the apparent resistance of CD8-/- to EAMG is not due to insufficient antibody-mediated complement activation.

CD8-/- mice have reduced frequencies of peripheral blood AChR+IgG2+ B cells

We have previously shown that the frequency of peripheral blood AChR+IgG2+ B cells is an indicator of EAMG disease severity (Chapter 4). To further characterize the extent of B cell activation in CD8-/- mice, we utilized the Alexa fluor-AChR flow cytometry assay to detect circulating AChR-specific B cells. Lymphocytes were gated on B220+ cells, and then expression of Ig and binding of AChR were compared (Figure 27).

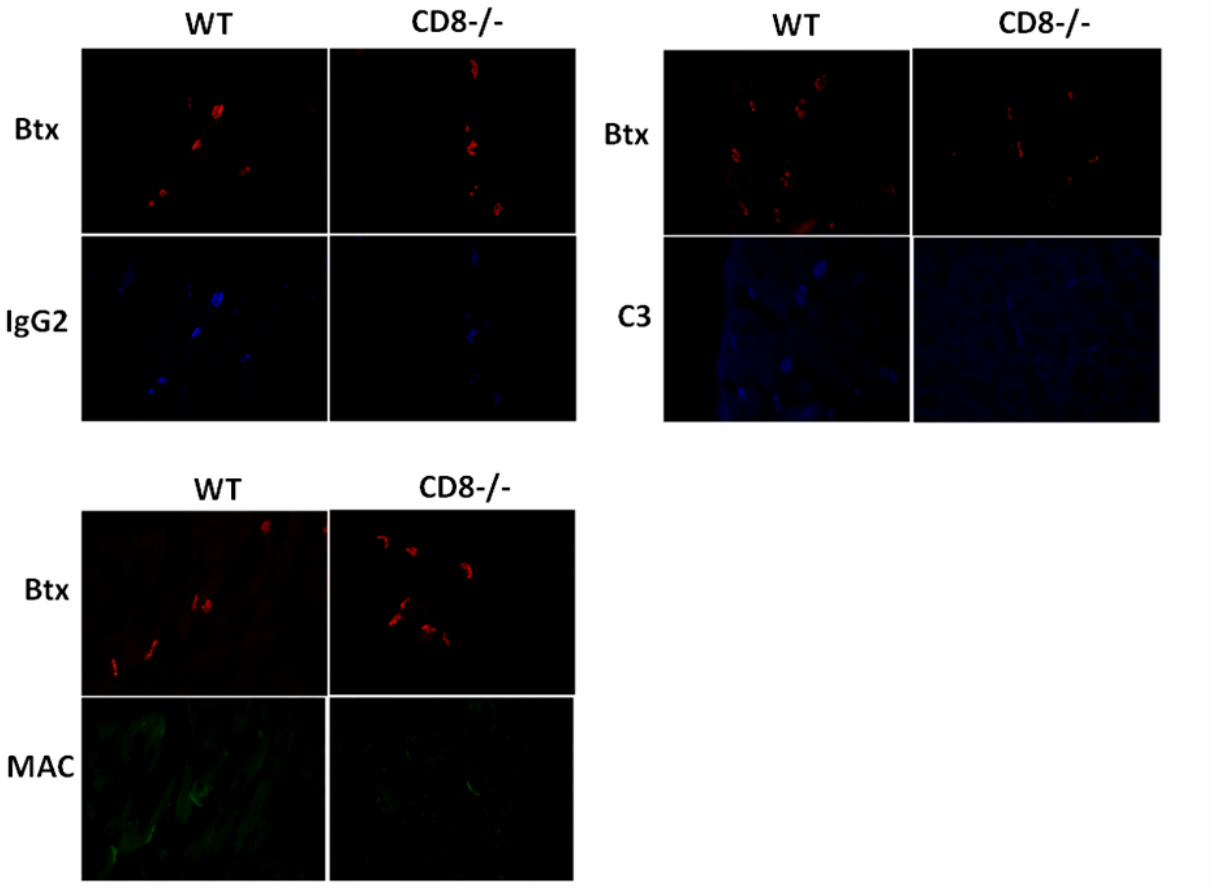

FIGURE 26: IgG2, C3, and MAC deposition detected in muscle of CD8-/- immunized mice. EAMG was induced in WT and CD8-/- C57BL/6 mice by multiple immunizations and euthanized on day 80 post-primary immunization. Control mice were unimmunized. Cryostat sections of right tricep muscle were co-stained with α-bungarotoxin (Btx) to identify AChR (red) and either anti-mouse IgG2 (blue), anti-mouse MAC (green), or anti-mouse C3 (blue). Data shown are representative of sections obtained from several mice from each group (n =5). Original 200 X magnification.

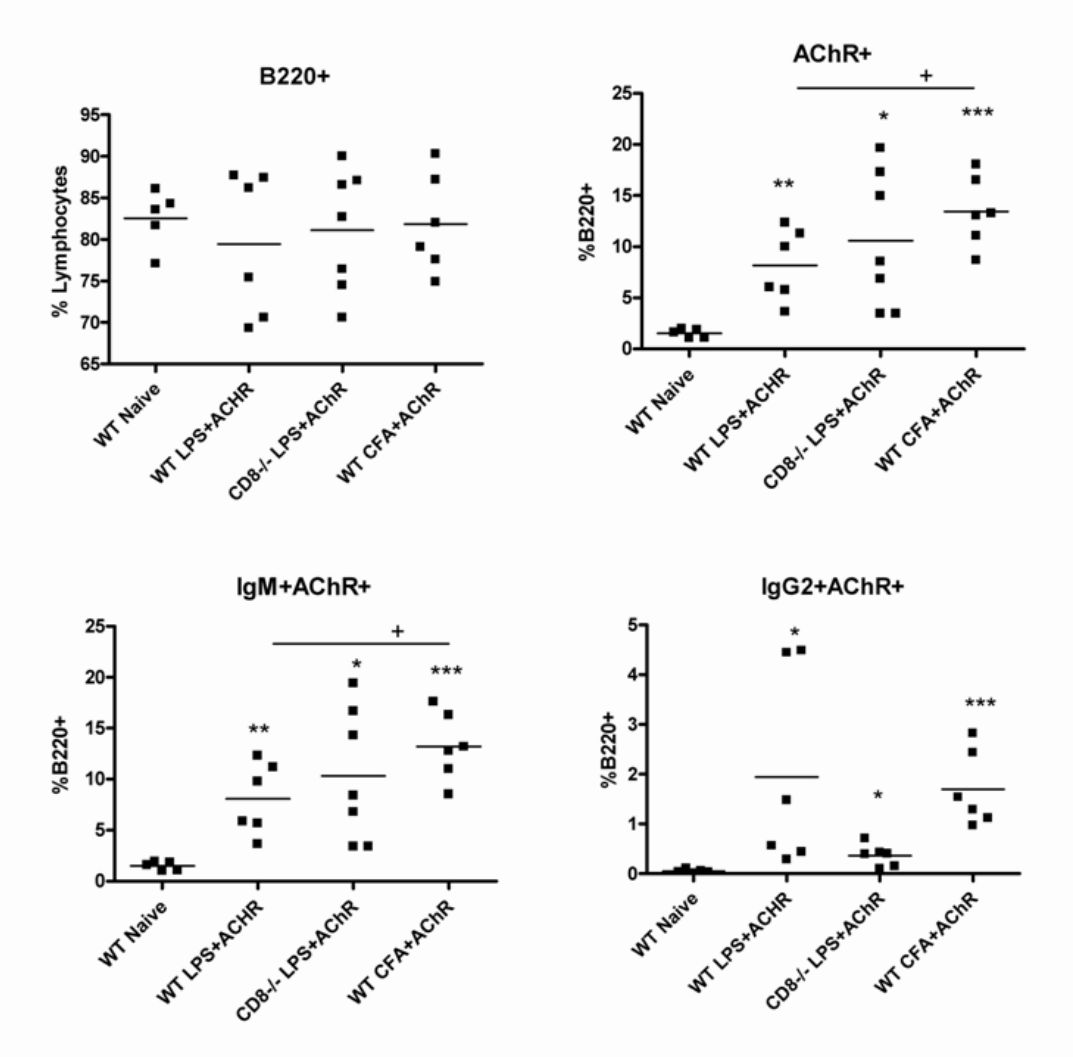

FIGURE 27: The frequencies of AChR-binding peripheral blood B cells are reduced in CD8-/- mice. Flow cytometry analysis of peripheral blood lymphocytes from 75 days post primary immunization. Cells were first gated on B220+ lymphocytes to characterize IgM or IgG2 expression and AChR binding. Mean frequency of B220+ lymphocytes, total AChR-binding B cells, IgM+ AChR-binding B cells and IgG2+ AChR-binding B cells (n=5-7), Student's *t*-test, * $p<0.05$, ** $p<.0.01$,***$P<0.001$.

There were no significant differences in the total frequencies of B cells (B220+ lymphocytes) present in blood of naïve, WT, and CD8-/- LPS-AChR immunized mice. All mice immunized with AChR regardless of genotype or adjuvant used had significantly elevated frequencies of AChR-binding B cells compared to naïve mice (Figure 27). Of interest, LPS-AChR immunized CD8-/- mice had lower mean frequencies of AChR-binding IgG2+ B cells than WT CFA-AChR and WT LPS-AChR immunized mice. These data indicate that CD8 deficiency has an effect on the survival of B cells in the periphery.

DISCUSSION

LPS-AChR immunization of CD8-/- mice led to the production of high affinity complement-binding isotypes of anti-AChR Abs (IgM and IgG2), which were detected near the NMJs of limb muscles. Despite the deposition of immune complexes in muscle, CD8-/- mice were resistant to the development of moderate or severe signs of EAMG. Taken together, these studies indicate that CD8+ T cells play a role in the pathogenesis of EAMG which is independent of Ab-mediated immune responses. Immunohistochemical staining of muscle at day 80 with anti-CD8 Ab failed to show the presence of CD8+ T cells in WT LPS-AChR immunized mice (data not shown). Furthermore, CD8+ T cells from patients with MG have poor proliferation responses to AChR and show little to no cytotoxic activity when cultured with human muscle cells. Therefore, it is unlikely that FAS-mediated or cytotoxic granule-killing of muscle cells is involved in the pathogenesis of MG, but these studies cannot rule out the possibility.

CD8+ T cells are producers of IFN–γ and TNF-α, which have been shown to play a role in the pathogenesis of MG (2, 109). It is possible that CD8-/- mice produce lower levels of these cytokines post immunization with LPS-AChR leading to reduced inflammation and a reduction in the clinical signs of EAMG. Others have shown that purified naïve human CD8+ T cells produced both IFN–γ and TNF-α when stimulated *in vitro* with LPS (110).

In this chapter, we show that CD8 deficiency led to a decrease in the frequency of peripheral blood AChR+IgG2+ B cells in LPS-AChR immunized mice. Previously we have shown that reduced frequencies of AChR+IgG2+ B cells corresponds with resistance to EAMG or improved clinical signs of disease (Chapter 4). Since anti-AChR Ab production was not altered in CD8-/- mice, these data further support the theory that pathogenic B cells contribute to the development of EAMG through functions other than Ab secretion. In Chapter 5, we have shown that CD4 deficiency led to an increase in peripheral blood AChR+ IgG2+ B cells in LPS-AChR immunized mice. Furthermore, CD4-/- mice immunized with CFA-AChR failed to secrete IgG2 yet have significant populations of circulating AChR+IgG2b+ B cells. In addition, our previous research has shown that Ab secretion does not correlate well with circulating B cell frequencies (Chapter 4). Taken together, these studies indicate that signals from CD8+ T cells may be important for the survival of circulating memory/effector B cells, but do not effect B cell differentiation into antibody secreting cells.

Chapter 7: Summary and Conclusions

The purpose of this dissertation was to develop a new model of EAMG using the T-independent adjuvant, LPS, to elucidate the signals required for the induction of pathogenic B cell Ab production (LPS-EAMG). Historically, EAMG is induced by immunization of mice with AChR emulsified in CFA (CFA-EAMG). In these studies, we have shown that immunization of mice with LPS and AChR emulsified in IFA induces clinical signs of EAMG, anti-AChR Ab production, pathogenic deposits at NMJ (IgG, C3, MAC), and loss of functional AChR in skeletal muscle. Immunization of mice with LPS alone but not CFA alone enhanced TLR4 expression on peripheral lymphocytes and the secretion of IgG2. These data suggested to us that the LPS-EAMG and CFA-EAMG may induce different immune mechanisms that trigger autoimmunity.

Next, we investigated the potential of LPS to induce antigen-specific B cell responses to AChR in WT and CD4-/- C57BL/6 mice. CD4-/- mice were resistant to the development of CFA-EAMG, but susceptible to the development of LPS-EAMG. The findings, accordingly have allowed us to identify an alternate cellular mechanism for disease induction. The CD4-/- mice in the LPS-EAMG model had significant amounts of high-affinity anti-AChR IgG2 antibody, immune complex deposits in muscle, and elevated sera levels of the B cell survival factor BAFF. Our results indicate that LPS abrogated tolerance in the LPS-EAMG model by inducing BAFF, while lowering the expression of co-stimulatory molecules CD40 and CD40L.

To further characterize B cell development we used a flow cytometric assay for the detection of peripheral blood AChR-specific B cells to characterize B cell phenotypes associated with EAMG. Alexa-conjugated AChR was used as a probe for AChR-specific B cells (B220+Ig+). Mice with EAMG have significantly elevated frequencies of AChR-specific IgG2+ and IgM+ B cells. The frequencies of AChR-specific B cells significantly correlated with the clinical grade of disease and loss of limb muscle strength, but not with the concentrations of plasma anti-AChR Igs. These results indicate that significantly elevated frequencies of AChR-specific peripheral blood B cells could be a potential biomarker for MG disease severity. The diagnostic use of this assay needs to be investigated further in patients with MG.

Both LPS-AChR and CFA-AChR immunized CD4-/- mice had higher mean frequencies of IgG expressing AChR-binding B cells than WT mice treated in the same manner. This difference was exacerbated in CFA-AChR immunized CD4-/- mice. However, B cells from CD4-/- mice immunized with CFA-AChR failed to differentiate into antibody secreting cells. These data suggest that the lack of anti-AChR IgG secretion by CFA-AChR immunized CD4-/- mice was not due to an inability to activate naïve B cells, inefficient CSR or deletion of autoreactive B cells. On the contrary, it appears that CD4 costimulation of B cells may actually inhibit the expansion of AChR-specific B cells and CSR to IgG2. Therefore, B cells from CFA-AChR immunized CD4-/- mice are either inhibited from differentiating into antibody secreting plasma cells or perhaps preferentially shunted into the memory B cell repertoire or are developmentally blocked from secreting Ab. However, LPS stimulation of B cells appears to overcome the

requirement of CD4 costimulation to differentiate into antibody secreting cells. These data confirmed that autoimmune development triggered by LPS or CFA occur by activation of distinct B cell differentiation pathways.

Since CD4+ T cell costimulation of B cells was not required for the development of EAMG, we then investigated the role of CD8+ T cells. LPS-AChR immunization of CD8-/- mice led to the production of high affinity complement-binding isotypes of anti-AChR Abs (IgM and IgG2), which were detected near the NMJs of limb muscles. Despite the deposition of immune complexes in muscle, CD8-/- mice were resistant to the development of moderate or severe signs of EAMG. CD8 deficiency led to a decrease in the frequency of peripheral blood AChR+IgG2+ B cells in LPS-AChR immunized mice. These studies indicate that signals from CD8+ T cells may be important for the survival of circulating memory/effector B cells, but do not effect B cell differentiation into antibody secreting cells. Taken together, CD8+ T cells may play a role in the pathogenesis of EAMG which is independent of Ab-mediated immune responses.

This dissertation contributes to our understanding of the mechanisms involved in the activation and differentiation of autoreactive B cells. Specifically, this body of work shows how potential triggers of autoimmunity by microbes effect the cellular requirements for the induction of EAMG and indicates that peripheral blood AChR+IgG2+ (or IgG1 in humans) B cells contribute to the pathogenesis of MG by means other than direct deposition of immune complexes in muscle.

REFERENCES

1. Drachman, D. B. 1994. Myasthenia gravis. *N Engl J Med* 330:1797-1810.
2. Marx, A. 1993. *Chapter 43. Myasthenia Gravis. Molecular Pathology of Autoimmune Diseases*. Feedman & Company, New York, NY.
3. Conti-Fine, B. M., M. Milani, and H. J. Kaminski. 2006. Myasthenia gravis: past, present, and future. *J Clin Invest* 116:2843-2854.
4. Willcox, N. 1993. Myasthenia gravis. *Curr Opin Immunol* 5:910-917.
5. Kaminski, H. J. 1998. Acetylcholine receptor epitopes in ocular myasthenia. *Ann N Y Acad Sci* 841:309-319.
6. Patrick, J., and J. Lindstrom. 1973. Autoimmune response to acetylcholine receptor. *Science* 180:871-872.
7. Satyamurti, S., D. B. Drachman, and F. Slone. 1975. Blockade of acetylcholine receptors: a model of myasthenia gravis. *Science* 187:955-957.
8. Toyka, K. V., D. B. Drachman, D. E. Griffin, A. Pestronk, J. A. Winkelstein, K. H. Fishbeck, and I. Kao. 1977. Myasthenia gravis. Study of humoral immune mechanisms by passive transfer to mice. *N Engl J Med* 296:125-131.
9. Lefvert, A. K., K. Bergstrom, G. Matell, P. O. Osterman, and R. Pirskanen. 1978. Determination of acetylcholine receptor antibody in myasthenia gravis: clinical usefulness and pathogenetic implications. *J Neurol Neurosurg Psychiatry* 41:394-403.

10. Drachman, D. B., R. N. Adams, L. F. Josifek, and S. G. Self. 1982. Functional activities of autoantibodies to acetylcholine receptors and the clinical severity of myasthenia gravis. *N Engl J Med* 307:769-775.

11. Hoch, W., J. McConville, S. Helms, J. Newsom-Davis, A. Melms, and A. Vincent. 2001. Auto-antibodies to the receptor tyrosine kinase MuSK in patients with myasthenia gravis without acetylcholine receptor antibodies. *Nat Med* 7:365-368.

12. Willcox, N., M. I. Leite, Y. Kadota, M. Jones, A. Meager, P. Subrahmanyam, B. Dasgupta, B. P. Morgan, and A. Vincent. 2008. Autoimmunizing mechanisms in thymoma and thymus. *Ann N Y Acad Sci* 1132:163-173.

13. Leite, M. I., M. Jones, P. Strobel, A. Marx, R. Gold, E. Niks, J. J. Verschuuren, S. Berrih-Aknin, F. Scaravilli, A. Canelhas, B. P. Morgan, A. Vincent, and N. Willcox. 2007. Myasthenia gravis thymus: complement vulnerability of epithelial and myoid cells, complement attack on them, and correlations with autoantibody status. *Am J Pathol* 171:893-905.

14. Bernasconi, P., M. Barberis, F. Baggi, L. Passerini, M. Cannone, E. Arnoldi, L. Novellino, F. Cornelio, and R. Mantegazza. 2005. Increased toll-like receptor 4 expression in thymus of myasthenic patients with thymitis and thymic involution. *Am J Pathol* 167:129-139.

15. Thangarajh, M., T. Masterman, L. Helgeland, U. Rot, M. V. Jonsson, G. E. Eide, R. Pirskanen, J. Hillert, and R. Jonsson. 2006. The thymus is a source of B-cell-

survival factors-APRIL and BAFF-in myasthenia gravis. *J Neuroimmunol* 178:161-166.

16. Kornstein, M. J., and G. G. DeBlois. 1995. *Pathology of the thymus and mediastinum* W.B. Saunders, Philadelphia, PA.

17. LeBien, T. W., and T. F. Tedder. 2008. B lymphocytes: how they develop and function. *Blood* 112:1570-1580.

18. Zettl, U. K., and E. Mix. 2006. Intravenous immunoglobulins in neurological diseases. *J Neurol* 253 Suppl 5:V1.

19. Mix, E., R. Goertsches, and U. K. Zett. 2006. Immunoglobulins--basic considerations. *J Neurol* 253 Suppl 5:V9-17.

20. Longo, N. S., and P. E. Lipsky. 2006. Why do B cells mutate their immunoglobulin receptors? *Trends Immunol* 27:374-380.

21. Carroll, M. C. 2004. The complement system in regulation of adaptive immunity. *Nat Immunol* 5:981-986.

22. Jacob, J., G. Kelsoe, K. Rajewsky, and U. Weiss. 1991. Intraclonal generation of antibody mutants in germinal centres. *Nature* 354:389-392.

23. Brack, C., M. Hirama, R. Lenhard-Schuller, and S. Tonegawa. 1978. A complete immunoglobulin gene is created by somatic recombination. *Cell* 15:1-14.

24. McHeyzer-Williams, M. G., M. J. McLean, P. A. Lalor, and G. J. Nossal. 1993. Antigen-driven B cell differentiation in vivo. *J Exp Med* 178:295-307.

25. O'Connor, B. P., M. W. Gleeson, R. J. Noelle, and L. D. Erickson. 2003. The rise and fall of long-lived humoral immunity: terminal differentiation of plasma cells in health and disease. *Immunol Rev* 194:61-76.

26. William, J., C. Euler, S. Christensen, and M. J. Shlomchik. 2002. Evolution of autoantibody responses via somatic hypermutation outside of germinal centers. *Science* 297:2066-2070.

27. Lopes-Carvalho, T., J. Foote, and J. F. Kearney. 2005. Marginal zone B cells in lymphocyte activation and regulation. *Curr Opin Immunol* 17:244-250.

28. Vincent, A. 1994. Aetiological factors in development of myasthenia gravis. *Adv Neuroimmunol* 4:355-371.

29. Jander, S., and G. Stoll. 2002. Increased serum levels of the interferon-gamma-inducing cytokine interleukin-18 in myasthenia gravis. *Neurology* 59:287-289.

30. Yoshikawa, H., K. Sato, S. Edahiro, Y. Furukawa, T. Maruta, K. Iwasa, H. Watanabe, S. Takaoka, Y. Suzuki, M. Takamori, and M. Yamada. 2006. Elevation of IL-12 p40 and its antibody in myasthenia gravis with thymoma. *J Neuroimmunol* 175:169-175.

31. Godessart, N., and S. L. Kunkel. 2001. Chemokines in autoimmune disease. *Curr Opin Immunol* 13:670-675.

32. Lennon, V. A., J. M. Lindstrom, and M. E. Seybold. 1975. Experimental autoimmune myasthenia: A model of myasthenia gravis in rats and guinea pigs. *J Exp Med* 141:1365-1375.

33. Wu, B., E. Goluszko, and P. Christadoss. 2001. Experimental autoimmune myasthenia gravis in the mouse. *Curr Protoc Immunol* Chapter 15:Unit 15 18.

34. Christadoss, P., R. Kaul, M. Shenoy, and E. Goluszko. 1995. Establishment of a mouse model of myasthenia gravis which mimics human myasthenia gravis pathogenesis for immune intervention. *Adv Exp Med Biol* 383:195-199.

35. Christadoss, P., M. Poussin, and C. Deng. 2000. Animal models of myasthenia gravis. *Clin Immunol* 94:75-87.

36. Bach, J. F. 2005. Infections and autoimmune diseases. *J Autoimmun* 25 Suppl:74-80.

37. Kamradt, T., R. Goggel, and K. J. Erb. 2005. Induction, exacerbation and inhibition of allergic and autoimmune diseases by infection. *Trends Immunol* 26:260-267.

38. Billiau, A., and P. Matthys. 2001. Modes of action of Freund's adjuvants in experimental models of autoimmune diseases. *J Leukoc Biol* 70:849-860.

39. Deitiker, P., T. Ashizawa, and M. Z. Atassi. 2000. Antigen mimicry in autoimmune disease. Can immune responses to microbial antigens that mimic acetylcholine receptor act as initial triggers of Myasthenia gravis? *Hum Immunol* 61:255-265.

40. Schwimmbeck, P. L., T. Dyrberg, D. B. Drachman, and M. B. Oldstone. 1989. Molecular mimicry and myasthenia gravis. An autoantigenic site of the acetylcholine receptor alpha-subunit that has biologic activity and reacts immunochemically with herpes simplex virus. *J Clin Invest* 84:1174-1180.

41. Stefansson, K., M. E. Dieperink, D. P. Richman, C. M. Gomez, and L. S. Marton. 1985. Sharing of antigenic determinants between the nicotinic acetylcholine receptor and proteins in Escherichia coli, Proteus vulgaris, and Klebsiella pneumoniae. Possible role in the pathogenesis of myasthenia gravis. *N Engl J Med* 312:221-225.

42. De Milito, A. 2004. B lymphocyte dysfunctions in HIV infection. *Curr HIV Res* 2:11-21.

43. Felice, K. J., F. J. DiMario, and S. R. Conway. 2005. Postinfectious myasthenia gravis: report of two children. *J Child Neurol* 20:441-444.

44. Finsterer, J. 2007. Myasthenia and neuroborreliosis with excessively high acetylcholine-receptor antibodies. *Scand J Infect Dis* 39:187-190.

45. Lalive, P. H., G. Allali, and A. Truffert. 2007. Myasthenia gravis associated with HTLV-I infection and atypical brain lesions. *Muscle Nerve* 35:525-528.

46. Verma, A., and J. Berger. 1995. Myasthenia gravis associated with dual infection of HIV and HTLV-I. *Muscle Nerve* 18:1355-1356.

47. Miller, S. I., R. K. Ernst, and M. W. Bader. 2005. LPS, TLR4 and infectious disease diversity. *Nat Rev Microbiol* 3:36-46.

48. Ishii, K. J., and S. Akira. 2007. Toll or toll-free adjuvant path toward the optimal vaccine development. *J Clin Immunol* 27:363-371.

49. Tough, D. F., S. Sun, and J. Sprent. 1997. T cell stimulation in vivo by lipopolysaccharide (LPS). *J Exp Med* 185:2089-2094.

50. Ehlers, M., H. Fukuyama, T. L. McGaha, A. Aderem, and J. V. Ravetch. 2006. TLR9/MyD88 signaling is required for class switching to pathogenic IgG2a and 2b autoantibodies in SLE. *J Exp Med* 203:553-561.

51. He, B., X. Qiao, and A. Cerutti. 2004. CpG DNA induces IgG class switch DNA recombination by activating human B cells through an innate pathway that requires TLR9 and cooperates with IL-10. *J Immunol* 173:4479-4491.

52. Chu, V. T., P. Enghard, G. Riemekasten, and C. Berek. 2007. In vitro and in vivo activation induces BAFF and APRIL expression in B cells. *J Immunol* 179:5947-5957.

53. Craxton, A., D. Magaletti, E. J. Ryan, and E. A. Clark. 2003. Macrophage- and dendritic cell--dependent regulation of human B-cell proliferation requires the TNF family ligand BAFF. *Blood* 101:4464-4471.

54. Litinskiy, M. B., B. Nardelli, D. M. Hilbert, B. He, A. Schaffer, P. Casali, and A. Cerutti. 2002. DCs induce CD40-independent immunoglobulin class switching through BLyS and APRIL. *Nat Immunol* 3:822-829.

55. Tuzun, E., B. G. Scott, H. Yang, B. Wu, E. Goluszko, M. Guigneaux, S. Higgs, and P. Christadoss. 2004. Circulating immune complexes augment severity of antibody-mediated myasthenia gravis in hypogammaglobulinemic RIIIS/J mice. *J Immunol* 172:5743-5752.

56. Granholm, N. A., and T. Cavallo. 1994. Long-lasting effects of bacterial lipopolysaccharide promote progression of lupus nephritis in NZB/W mice. *Lupus* 3:507-514.

57. Kong, Y. C. 2007. Experimental autoimmune thyroiditis in the mouse. *Curr Protoc Immunol* Chapter 15:Unit 15 17.

58. Berman, P. W., and J. Patrick. 1980. Experimental myasthenia gravis. A murine system. *J Exp Med* 151:204-223.

59. Milani, M., N. Ostlie, H. Wu, W. Wang, and B. M. Conti-Fine. 2006. CD4+ T and B cells cooperate in the immunoregulation of Experimental Autoimmune Myasthenia Gravis. *J Neuroimmunol* 179:152-162.

60. Wu, B., C. Deng, E. Goluszko, and P. Christadoss. 1997. Tolerance to a dominant T cell epitope in the acetylcholine receptor molecule induces epitope spread and suppresses murine myasthenia gravis. *J Immunol* 159:3016-3023.

61. Lenert, P., A. Goeken, B. S. Handwerger, and R. F. Ashman. 2003. Innate immune responses in lupus-prone Palmerston North mice: differential responses to LPS and bacterial DNA/CpG oligonucleotides. *J Clin Immunol* 23:202-213.

62. Yoshino, S., E. Sasatomi, and M. Ohsawa. 2000. Bacterial lipopolysaccharide acts as an adjuvant to induce autoimmune arthritis in mice. *Immunology* 99:607-614.

63. Damotte, D., C. Goulvestre, J. Charreire, and C. Carnaud. 2003. LPS and Freund's adjuvant initiate different inflammatory circuits in experimental autoimmune thyroiditis. *Eur Cytokine Netw* 14:52-59.

64. Shi, F. D., H. G. Ljunggren, and N. Sarvetnick. 2001. Innate immunity and autoimmunity: from self-protection to self-destruction. *Trends Immunol* 22:97-101.

65. Cohen-Kaminsky, S., R. M. Delattre, O. Devergne, P. Rouet, D. Gimond, S. Berrih-Aknin, and P. Galanaud. 1991. Synergistic induction of interleukin-6 production and gene expression in human thymic epithelial cells by LPS and cytokines. *Cell Immunol* 138:79-93.

66. Gronseth, G. S., and R. J. Barohn. 2000. Practice parameter: thymectomy for autoimmune myasthenia gravis (an evidence-based review): report of the Quality Standards Subcommittee of the American Academy of Neurology. *Neurology* 55:7-15.

67. Levinson, A. I., Y. Zheng, G. Gaulton, J. Moore, C. H. Pletcher, D. Song, and L. M. Wheatley. 2003. A new model linking intrathymic acetylcholine receptor expression and the pathogenesis of myasthenia gravis. *Ann N Y Acad Sci* 998:257-265.

68. Savino, W. 2006. The thymus is a common target organ in infectious diseases. *PLoS Pathog* 2:e62.

69. Zisimopoulou, P., G. Lagoumintzis, K. Kostelidou, K. Bitzopoulou, G. Kordas, N. Trakas, K. Poulas, and S. J. Tzartos. 2008. Towards antigen-specific apheresis of pathogenic autoantibodies as a further step in the treatment of myasthenia gravis by plasmapheresis. *J Neuroimmunol* 201-202:95-103.

70. Bufler, J., R. Pitz, M. Czep, M. Wick, and C. Franke. 1998. Purified IgG from seropositive and seronegative patients with mysasthenia gravis reversibly blocks currents through nicotinic acetylcholine receptor channels. *Ann Neurol* 43:458-464.

71. Vincent, A., and D. B. Drachman. 2002. Myasthenia gravis. *Adv Neurol* 88:159-188.

72. Fambrough, D. M., D. B. Drachman, and S. Satyamurti. 1973. Neuromuscular junction in myasthenia gravis: decreased acetylcholine receptors. *Science* 182:293-295.

73. Freeman, S. S., A. G. Engel, and D. B. Drachman. 1976. Experimental acetylcholine blockade of the neuromuscular junction. Effects on end plate and muscle fiber ultrastructure. *Ann N Y Acad Sci* 274:46-59.

74. Lindstrom, J. M., M. E. Seybold, V. A. Lennon, S. Whittingham, and D. D. Duane. 1976. Antibody to acetylcholine receptor in myasthenia gravis. Prevalence, clinical correlates, and diagnostic value. *Neurology* 26:1054-1059.

75. Vincent, A., and J. Newsom-Davis. 1985. Acetylcholine receptor antibody as a diagnostic test for myasthenia gravis: results in 153 validated cases and 2967 diagnostic assays. *J Neurol Neurosurg Psychiatry* 48:1246-1252.

76. Christadoss, P., J. Lindstrom, S. Munro, and N. Talal. 1985. Muscle acetylcholine receptor loss in murine experimental autoimmune myasthenia gravis: correlated with cellular, humoral and clinical responses. *J Neuroimmunol* 8:29-41.

77. Krolick, K. A., T. E. Zoda, and P. A. Thompson. 1994. Examination of characteristics that may distinguish disease-causing from benign AChR-reactive antibodies in experimental autoimmune myasthenia gravis. *Adv Neuroimmunol* 4:475-493.

78. Doucett, V. P., W. Gerhard, K. Owler, D. Curry, L. Brown, and N. Baumgarth. 2005. Enumeration and characterization of virus-specific B cells by multicolor flow cytometry. *J Immunol Methods* 303:40-52.

79. Leyendeckers, H., M. Odendahl, A. Lohndorf, J. Irsch, M. Spangfort, S. Miltenyi, N. Hunzelmann, M. Assenmacher, A. Radbruch, and J. Schmitz. 1999. Correlation analysis between frequencies of circulating antigen-specific IgG-bearing memory B cells and serum titers of antigen-specific IgG. *Eur J Immunol* 29:1406-1417.

80. Newman, J., J. S. Rice, C. Wang, S. L. Harris, and B. Diamond. 2003. Identification of an antigen-specific B cell population. *J Immunol Methods* 272:177-187.

81. Yamagami, J., H. Takahashi, T. Ota, and M. Amagai. 2008. Genetic characterization of human Dsg3-specific B cells isolated by flow cytometry from the peripheral blood of patients with pemphigus vulgaris. *J Dermatol Sci* 52:98-107.

82. Christadoss, P. 1988. C5 gene influences the development of murine myasthenia gravis. *J Immunol* 140:2589-2592.

83. Rojas, O. L., C. F. Narvaez, H. B. Greenberg, J. Angel, and M. A. Franco. 2008. Characterization of rotavirus specific B cells and their relation with serological memory. *Virology* 380:234-242.

84. Dedhia, V., E. Goluszko, B. Wu, C. Deng, and P. Christadoss. 1998. The effect of B cell deficiency on the immune response to acetylcholine receptor and the

development of experimental autoimmune myasthenia gravis. *Clin Immunol Immunopathol* 87:266-275.

85. Li, H., F. D. Shi, B. He, M. Bakheit, B. Wahren, A. Berglof, K. Sandstedt, and H. Link. 1998. Experimental autoimmune myasthenia gravis induction in B cell-deficient mice. *Int Immunol* 10:1359-1365.

86. Sahashi, K., A. G. Engel, E. H. Lambert, and F. M. Howard, Jr. 1980. Ultrastructural localization of the terminal and lytic ninth complement component (C9) at the motor end-plate in myasthenia gravis. *J Neuropathol Exp Neurol* 39:160-172.

87. Browning, J. L. 2006. B cells move to centre stage: novel opportunities for autoimmune disease treatment. *Nat Rev Drug Discov* 5:564-576.

88. Christadoss, P., J. M. Lindstrom, N. Talal, C. R. Duvic, A. Kalantri, and M. Shenoy. 1986. Immune response gene control of lymphocyte proliferation induced by acetylcholine receptor-specific helper factor derived from lymphocytes of myasthenic mice. *J Immunol* 137:1845-1849.

89. Kaul, R., M. Shenoy, E. Goluszko, and P. Christadoss. 1994. Major histocompatibility complex class II gene disruption prevents experimental autoimmune myasthenia gravis. *J Immunol* 152:3152-3157.

90. Zhang, G. X., B. G. Xiao, M. Bakhiet, P. van der Meide, H. Wigzell, H. Link, and T. Olsson. 1996. Both CD4+ and CD8+ T cells are essential to induce experimental autoimmune myasthenia gravis. *J Exp Med* 184:349-356.

91. Poussin, M. A., E. Tuzun, E. Goluszko, B. G. Scott, H. Yang, J. U. Franco, and P. Christadoss. 2003. B7-1 costimulatory molecule is critical for the development of experimental autoimmune myasthenia gravis. *J Immunol* 170:4389-4396.

92. Shi, F. D., B. He, H. Li, D. Matusevicius, H. Link, and H. G. Ljunggren. 1998. Differential requirements for CD28 and CD40 ligand in the induction of experimental autoimmune myasthenia gravis. *Eur J Immunol* 28:3587-3593.

93. Castigli, E., S. A. Wilson, S. Scott, F. Dedeoglu, S. Xu, K. P. Lam, R. J. Bram, H. Jabara, and R. S. Geha. 2005. TACI and BAFF-R mediate isotype switching in B cells. *J Exp Med* 201:35-39.

94. Genestier, L., M. Taillardet, P. Mondiere, H. Gheit, C. Bella, and T. Defrance. 2007. TLR agonists selectively promote terminal plasma cell differentiation of B cell subsets specialized in thymus-independent responses. *J Immunol* 178:7779-7786.

95. Dempsey, P. W., M. E. Allison, S. Akkaraju, C. C. Goodnow, and D. T. Fearon. 1996. C3d of complement as a molecular adjuvant: bridging innate and acquired immunity. *Science* 271:348-350.

96. Lyubchenko, T., J. M. Dal Porto, V. M. Holers, and J. C. Cambier. 2007. Cutting edge: Complement (C3d)-linked antigens break B cell anergy. *J Immunol* 179:2695-2699.

97. Scott, B. G., H. Yang, E. Tuzun, C. Dong, R. A. Flavell, and P. Christadoss. 2004. ICOS is essential for the development of experimental autoimmune myasthenia gravis. *J Neuroimmunol* 153:16-25.

98. Rathmell, J. C., M. P. Cooke, W. Y. Ho, J. Grein, S. E. Townsend, M. M. Davis, and C. C. Goodnow. 1995. CD95 (Fas)-dependent elimination of self-reactive B cells upon interaction with CD4+ T cells. *Nature* 376:181-184.

99. Rathmell, J. C., and C. C. Goodnow. 1995. Autoimmunity. The Fas track. *Curr Biol* 5:1218-1221.

100. Herve, M., I. Isnardi, Y. S. Ng, J. B. Bussel, H. D. Ochs, C. Cunningham-Rundles, and E. Meffre. 2007. CD40 ligand and MHC class II expression are essential for human peripheral B cell tolerance. *J Exp Med* 204:1583-1593.

101. Ragheb, S., R. Lisak, R. Lewis, G. Van Stavern, F. Gonzales, and K. Simon. 2008. A potential role for B-cell activating factor in the pathogenesis of autoimmune myasthenia gravis. *Arch Neurol* 65:1358-1362.

102. Thien, M., T. G. Phan, S. Gardam, M. Amesbury, A. Basten, F. Mackay, and R. Brink. 2004. Excess BAFF rescues self-reactive B cells from peripheral deletion and allows them to enter forbidden follicular and marginal zone niches. *Immunity* 20:785-798.

103. Walter, U., and P. Santamaria. 2005. CD8+ T cells in autoimmunity. *Curr Opin Immunol* 17:624-631.

104. Berg, R. E., and J. Forman. 2006. The role of CD8 T cells in innate immunity and in antigen non-specific protection. *Curr Opin Immunol* 18:338-343.

105. Seder, R. A., and G. G. Le Gros. 1995. The functional role of CD8+ T helper type 2 cells. *J Exp Med* 181:5-7.

106. Zozulya, A. L., and H. Wiendl. 2008. The role of CD8 suppressors versus destructors in autoimmune central nervous system inflammation. *Hum Immunol* 69:797-804.

107. Shenoy, M., R. Kaul, E. Goluszko, C. David, and P. Christadoss. 1994. Effect of MHC class I and CD8 cell deficiency on experimental autoimmune myasthenia gravis pathogenesis. *J Immunol* 153:5330-5335.

108. Hutchings, P. R., S. Verma, J. M. Phillips, S. Z. Harach, S. Howlett, and A. Cooke. 1999. Both CD4(+) T cells and CD8(+) T cells are required for iodine accelerated thyroiditis in NOD mice. *Cell Immunol* 192:113-121.

109. Duan, R. S., H. B. Wang, J. S. Yang, B. Scallon, H. Link, and B. G. Xiao. 2002. Anti-TNF-alpha antibodies suppress the development of experimental autoimmune myasthenia gravis. *J Autoimmun* 19:169-174.

110. Komai-Koma, M., D. S. Gilchrist, and D. Xu. 2009. Direct recognition of LPS by human but not murine CD8+ T cells via TLR4 complex. *Eur J Immunol* 39:1564-1572.

VITA

Windy Allman was born in Toms River, New Jersey on June 25, 1979 to William and Mary Ellen Allman. Windy is the youngest of six children which include; Joseph, William, Erica, Stephen and Hope Allman. In May 2001, she received a Bachelor of Science degree in neuroscience with a minor in biochemistry from the University of Scranton located in Pennsylvania. She received training as a research technician at the University of Texas Southwestern Medical Center and the Baylor Institute for Immunology Research in Dallas, Texas. She then joined the Ph.D. program in Microbiology and Immunology at the University of Texas Medical Branch at Galveston (UTMB) in 2005.

During her graduate training at UTMB, Windy has received several awards including: Association Francaise contre les Myopathies (AFM) Fellowship, James W. McLaughlin Collogium Travel Award (2007&2008), the Myasthenia Gravis Foundation of America (MGFA) Henry R. Viets Fellowship (2007-2008).

Upon completing her Ph.D., Windy has accepted a post-doctoral Oak Ridge Institute for Science and Education fellowship to perform research under the direction of Dr. Mustafa Akkoyunlu at the Center for Biologics Evaluation and Research (CBER) division of the U.S. Food and Drug Administration in Bethesda, MD.

PUBLICATIONS

Allman, W., Qi, H., Saini, S.S., Li, J., Christadoss, P. CD4 costimulation is not required in a novel LPS-enhances model of myasthenia gravis. Submitted (2009).

Allman, W., Saini, S.S., Christadoss, P. Frequency of acetylcholine receptor specific B cells correlates with experimental myasthenia gravis severity. Submitted (2009).

Li, J., Qi, H., Tuzun, E., **Allman, W.**, Yilmaz, V., Saini, S.S., Deymeer, F., Surahan-Direskeneli, G., Christadoss, P. 2009. Mannose-binding lectin pathway is not involved in myasthenia gravis pathogenesis. *J Neuroimmunol* 1-2: 40-45.

Chaussabel, D., Quinn, C., Shen, J., Patel, P., Glaser, C., Baldwin, N., Stichweh, D., Blankenship, D., Li, L., Munagala, I., Bennett, L., Allantaz, F., Mejias, A., Ardura, M., Kaizer, E., Monnet, L., **Allman, W.**, Randall, H., Johnson, D., Lanier, A., Punaro, M., Wittkowski, K., White, P., Fay, J., Klintmalm, G., Ramilo, O., Palucka, A.K., Banchereau, J., Pascual, V. 2008. A Modular Analysis Framework for Blood Genomics Studies: Application to Systemic Lupus Erythematosus. *Immunity* 29: 150-164.

Qi, H., Tuzun, E., **Allman, W.**, Saini, S.S., Christadoss, P. 2008. C5a is not involved in experimental autoimmune myasthenia gravis. *J Neuroimmunol* 196:101-106.

Li, J., Tuzun, E., Wu, X., Qi, H., **Allman, W**., Saini, S.S., Christadoss, P. 2008. Inhibitory IgG receptor FcγRIIB promotes experimental autoimmune myasthenia gravis pathogenesis by stimulating IL-6 and IL-10 production. *J Neuroimmunol* 194: 44-53.

Yang, H., Wu, B., Tuzun, E., Saini, S.S., Li, J., **Allman, W**., Higgs, S., Xiao. T.L., Christadoss, P. 2007. A New Model of Autoimmune Ocular Myasthenia Gravis. *Invest Ophthalmol Vis Sci* 48: 5101-5111.

Allantaz, F., Chaussabel, D., Stichweh, D., Bennett, L., **Allman, W.,** Mejias, A., Ardura, M., Chung, W., Wise, C., Palucka, K., Ramilo, O., Puraro, M., Banchereau, J., Pascual, V. 2007. Blood Leukocyte Microarrays Diagnose Systemic Juvenile Idiopathic Arthritis and follow the response to IL-1 Blockade. *J Exp Med* 204: 2134-2144.

Ramilo O, **Allman W**, Chung W, Mejias A, Ardura M, Glaser C, Wittkowski K, Piqueras B, Banchereau J, Palucka A, Chaussabel D. 2006. Gene Expression Patterns in Blood Leukocytes Discriminate Patients with acute Infections. *Blood* 109: 2066-2077.

Chaussabel, D, **Allman, W**, Mejias, A, Chung, W, Bennett,, L, Ramilo, O, Pascual, V., Palucka, K, Banchereau, J. 2005. Analysis of Significance Patterns Identifies Ubiquitous

and Disease-Specific Gene-Expression Signatures in Patient Peripheral Blood Leukocytes. *Ann NY Acad Sci* 1062: 146-1054.